Zoonotic Source Attribution of *Salmonella enterica* Serotype Typhimurium Using Genomic Surveillance Data, United States

Shaokang Zhang, Shaoting Li, Weidong Gu, Henk den Bakker, Dave Boxrud, Angie Taylor, Chandler Roe, Elizabeth Driebe, David M. Engelthaler, Marc Allard, Eric Brown, Patrick McDermott, Shaohua Zhao, Beau B. Bruce, Eija Trees, Patricia I. Fields, Xiangyu Deng

Increasingly, routine surveillance and monitoring of foodborne pathogens using whole-genome sequencing is creating opportunities to study foodborne illness epidemiology beyond routine outbreak investigations and case–control studies. Using a global phylogeny of *Salmonella enterica* serotype Typhimurium, we found that major livestock sources of the pathogen in the United States can be predicted through whole-genome sequencing data. Relatively steady rates of sequence divergence in livestock lineages enabled the inference of their recent origins. Elevated accumulation of lineage-specific pseudogenes after divergence from generalist populations and possible metabolic acclimation in a representative swine isolate indicates possible emergence of host adaptation. We developed and retrospectively applied a machine learning Random Forest classifier for genomic source prediction of *Salmonella* Typhimurium that correctly attributed 7 of 8 major zoonotic outbreaks in the United States during 1998–2013. We further identified 50 key genetic features that were sufficient for robust livestock source prediction.

Each year, 9.4 million episodes of foodborne illness occur in the United States (*1*). According to the Centers for Disease Control and Prevention, ≈95% of these infections are sporadic, nonoutbreak cases for which specific food exposures and contamination sources remain difficult to determine. The lack of source information for most foodborne infections substantially challenges understanding of the epidemiology of foodborne illnesses and development of intervention measures for their prevention and mitigation. Routine use of whole-genome sequencing (WGS) for foodborne illness surveillance and pathogen monitoring has created a large and quickly expanding wealth of genomes and associated metadata. Much of these data remain largely untapped beyond routine outbreak investigation.

Salmonella enterica is one of the most prevalent foodborne pathogens worldwide, causing >1 million human cases and an economic burden of $3.7 billion annually in the United States alone (*1*,*2*). *S. enterica* serotype Typhimurium is one of the most prevalent causes of human salmonellosis in many countries, including the United States (*3*). *Salmonella* Typhimurium strains display a broad host range and varying degrees of host adaptation (*4*). Diverse subtypes have caused emerging epidemics in recent decades. First isolated in the early 1980s in the United Kingdom, multidrug-resistant *Salmonella* Typhimurium definitive type 104 spread from cattle to other livestock in the country before its global dissemination during the 1990s (*5*). *Salmonella* Typhimurium sequence type (ST) 313 emerged ≈40–50 years ago in sub-Saharan Africa (*6*); its regional spread was linked to invasive disease symptoms and coincided with an HIV pandemic (*6*,*7*). The high prevalence, diverse reservoirs, and dynamic epidemiology of *Salmonella* Typhimurium have made it a paradigm for studying host specificity (*8*) and zoonotic colonization (*9*). Knowing the contribution of major sources of human illness caused by specific pathogens is critical for identifying, evaluating, and prioritizing public health intervention strategies (*10*). Microbiological source attribution relying on subtyping has shown some promise, such as a source attribution model from Denmark based on *Salmonella*

Author affiliations: University of Georgia Center for Food Safety, Griffin, Georgia, USA (S. Zhang, S. Li, H. den Bakker, X. Deng); Centers for Disease Control and Prevention, Atlanta, Georgia, USA (W. Gu, B.B. Bruce, E. Trees, P.I. Fields); Minnesota Department of Health, St. Paul, Minnesota, USA (D. Boxrud, A. Taylor); Translational Genomics Research Institute, Flagstaff, Arizona, USA (C. Roe, E. Driebe, D.M. Engelthaler); US Food and Drug Administration, College Park, Maryland, USA (M. Allard, E.W. Brown); US Food and Drug Administration, Laurel, Maryland, USA (P. McDermott, S. Zhao)

DOI: https://doi.org/10.3201/eid2501.180835

serotyping and phage typing (*11*). However, more recent models continued to use traditional phenotypes for *Salmonella* source attribution (*12*). The usefulness of more discriminating molecular subtyping for *Salmonella* source attribution has not been established (*12*).

We hypothesized that microbiological source attribution could be improved by an evolutionary understanding of pathogen populations and a mechanistic inquiry into their source association. We investigated zoonotic source attribution of *Salmonella* Typhimurium under an extensive phylogenomic framework by including a large collection of isolates from 3 major US laboratory surveillance and monitoring programs. We examined genotypic characteristics and metabolic profiles to assess livestock host adaptation and production environment colonization. Machine learning enabled comprehensive and high-resolution screening for key genetic indicators of source association throughout *Salmonella* Typhimurium genomes.

Materials and Methods

To study the population structure of *Salmonella* Typhimurium and its monophasic variant (I 4,[5],12:i:-), we first sequenced (n = 127) or collected (n = 1,140) 1,267 *Salmonella* Typhimurium genomes (Appendix 1 Table 1, https://wwwnc.cdc.gov/EID/article/25/1/18-0835-App1.xlsx; Appendix 2 section 1, https://wwwnc.cdc.gov/EID/article/25/1/18-0835-App1.pdf), comprising 4 sets of genomes. First, we selected human isolates from outbreak and sporadic cases in the United States during 1949–2014 (n = 127, sequenced for this study) to represent diverse pulsed-field gel electrophoresis patterns (n = 51) and multilocus variable-number tandem-repeat analysis patterns (n = 16, for isolates of known pattern) of *Salmonella* Typhimurium as surveyed by PulseNet USA during 1998–2014 (*13*). Second, we chose genomes in the GenomeTrakr database (*14*) as of September 2015 (n = 907) from food, environmental, and wild and livestock animal sources in the United States, Europe, South America, Asia, and Africa. Third, we included retail meat isolates sampled by the US National Antimicrobial Resistance Monitoring System (n = 157). Finally, we compiled other reported *Salmonella* Typhimurium genomes, including human ST313 isolates from sub-Saharan Africa (n = 76) (*6*). Publicly available genomes were confirmed to be *Salmonella* Typhimurium by SeqSero (*15*).

Overall metabolic potentials of 6 randomly selected representative isolates from 6 major population groups (Figure 1; Appendix 1 Table 2) were evaluated by Phenotype Microarrays (Biolog, https://biolog.com) (Appendix 2 section 8). Principal component analysis was conducted using Phenotype Microarrays results. Phylogenetic analysis, temporal signal screening and most recent common ancestor (MRCA) dating, and putative pseudogene identification

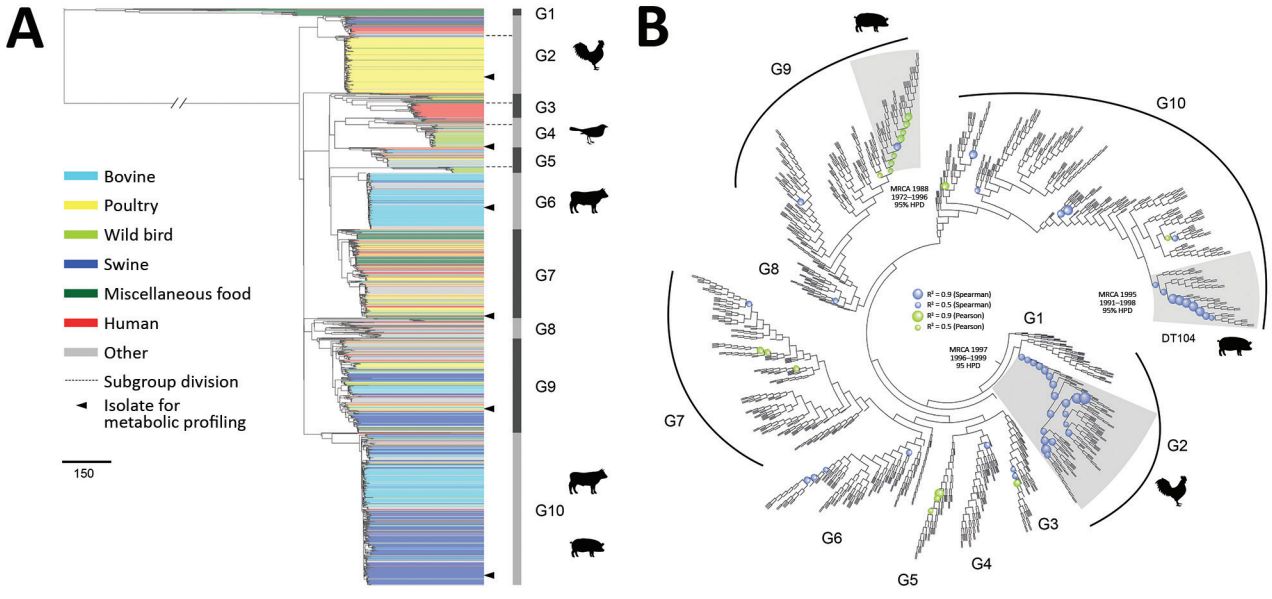

Figure 1. Phylogenetic structure of 1,267 *Salmonella enterica* serotype Typhimurium isolates. A) Maximum-likelihood phylogeny from 46 US states and 39 other countries. The tree was rooted at midpoint. Ten major population groups (G1–G10) were delineated. Each dashed line shows the division of subgroups in G2, G3, G4, and G5 (e.g., G2a and G2b). Each isolate is color coded by source. Arrowheads indicate isolates selected for metabolic profiling using Phenotype Microarrays (Biolog, https://biolog.com). Scale bar indicates number of single-nucleotide polymorphisms. B) Circular cladogram of the same maximum-likelihood phylogeny of the 1,267 isolates. Colored circles indicate internal nodes that had a squared coefficient (R^2) of the Spearman or Pearson correlation between isolation years and branch lengths >0.4. The sizes of the circle are proportional to the values of R^2 (0.0–0.9). Clades identified to exhibit temporal signals of single-nucleotide polymorphisms accumulation are shaded in gray. The inferred MRCA age of each clade is shown. HPD, highest posterior density; MRCA, most recent common ancestor.

were performed (Appendix 2 sections 2–4). A Random Forest classifier (https://www.stat.berkeley.edu/~breiman/randomforest2001.pdf) was built to predict zoonotic sources of *Salmonella* Typhimurium genomes (Appendix 2 sections 5, 6).

Results

Population Structure

We constructed a maximum-likelihood phylogeny of the 1,267 isolates based on single-nucleotide polymorphisms (SNPs) identified in the core genome alignments (Figure 1, panel A). We determined 39,562 single-nucleotide variable sites from the alignment. We excluded 154 genome segments potentially involved in recombination from the alignment and SNP identification. The recombinant regions (Appendix 1 Table 3) accounted for 269,366 nt (5.6%) of a typical *Salmonella* Typhimurium genome (4.8 Mb).

Bayesian analysis of the population structure delineated 10 population groups, designated G1–10 (Figure 1, panel A). Most population groups were monophyletic, except G5 and G8. G1 represented a highly divergent population (>9,000 SNPs) from other population groups and contained a high proportion (68.8%) of isolates from seafood, especially from Asia. Human clinical and miscellaneous food isolates (see source classification in Appendix 2 section 5) were widely distributed among population groups; clinical and food isolates were found in every group, except we found no food isolates in G6. Several groups contained major clades associated with particular sources, including G2b with poultry, G4b and G5b with wild birds, G6 with bovine, and G10 with swine and bovine sources (Figure 1, panel A; Appendix 1 Table 4). Other population groups included isolates from diverse sources. G7 accounted for all the aforementioned sources and had more human and food isolates than any other group. Representing 15.4% of the *Salmonella* Typhimurium collection, G7 had 21.6% and 40.2% of all human and food isolates. Eight major foodborne outbreaks during 1998–2012 were included. Of those, 5 were represented by isolates in G7: a 2006 picnic-associated outbreak in the United States, a 2009 multistate peanut butter–associated outbreak in the United States, a 2009 shredded lettuce–associated outbreak in the western United States and Canada, a 2010–2011 multistate alfalfa sprout–associated outbreak in the United States, and a 2012 multistate cantaloupe-associated outbreak in the United States.

To investigate the temporal history of *Salmonella* Typhimurium lineages, we searched temporal signals of SNP accumulation throughout the phylogeny by screening every internal node for strong correlation between isolation years and branch lengths (Figure 1, panel B). Although the entire phylogeny exhibited an overall weak temporal signal (R^2 <0.2), 3 clades showed moderate temporal signals (R^2 >0.4), permitting robust age inference of their MRCA. All 3 clades were associated with livestock and originated around the 1990s (Appendix 1 Table 5).

Differential Abundance of Putative Pseudogenes Among Recently Diverged Clades

We identified putative disruptive mutations (pseudogenes) in each *Salmonella* Typhimurium genome. Pseudogenes were most abundant in the sub-Saharan ST313 clade (G3b) and clades associated with wild birds (G4b and G5b) and seafood (G1). In multiple cases, we found significant differences ($p<0.01$) in pseudogene abundance between 2 recently diverged clades from a common ancestor; 1 comprised isolates from diverse sources and the other was associated predominantly with a particular source, such as wild birds (G4b), livestock (G2b, G6, and G10), and human ST313 cases in Africa (G3b) (Figure 2, panel A). We consistently observed elevated pseudogene accumulation in the source-associated and putatively host-adapted clades (Appendix 2 section 7). Most of these pseudogenes were clade-specific (Figure 2, panel B), suggesting they emerged and accumulated independently in different clades.

Differential Metabolic Potentials Among Representative Isolates

We characterized metabolic profiles of 6 representative human and animal isolates from 6 US population groups (G2b, G4b, G6, G7, G9, and G10) using Biolog Phenotype Microarrays comprising substrates of carbon, nitrogen, sulfur, and phosphorus sources. We found evidence for differential metabolic activity between any 2 isolates for 189 of the 384 substrates tested (Appendix 1 Table 2). Principal component analysis on metabolic activities suggested that a wild bird isolate (STM223) from G4b and swine isolate from G10 (STM712) deviated from each other and the rest of the isolates because of deficiency in using multiple substrates (Figure 2, panel C). Compared with a human isolate from G9 (STM988), the wild bird isolate showed reduced metabolic activity for 182 substrates and the swine isolate for 132 substrates. Some of these deficiencies correlated with the putative pseudogenes and nonsynonymous SNPs (Appendix 2 section 8).

Source Prediction Using WGS

To evaluate *Salmonella* Typhimurium source prediction using WGS, we updated the *Salmonella* Typhimurium genome collection (initially 1,267 genomes) by 1) adding 939 genomes that became available in GenomeTrakr during September 2015–January 2017; 2) sequencing another 11 isolates from 5 outbreaks with confirmed livestock origin in the United States during 2007–2013, which, together with 6 livestock isolates from 3 outbreaks in the original dataset,

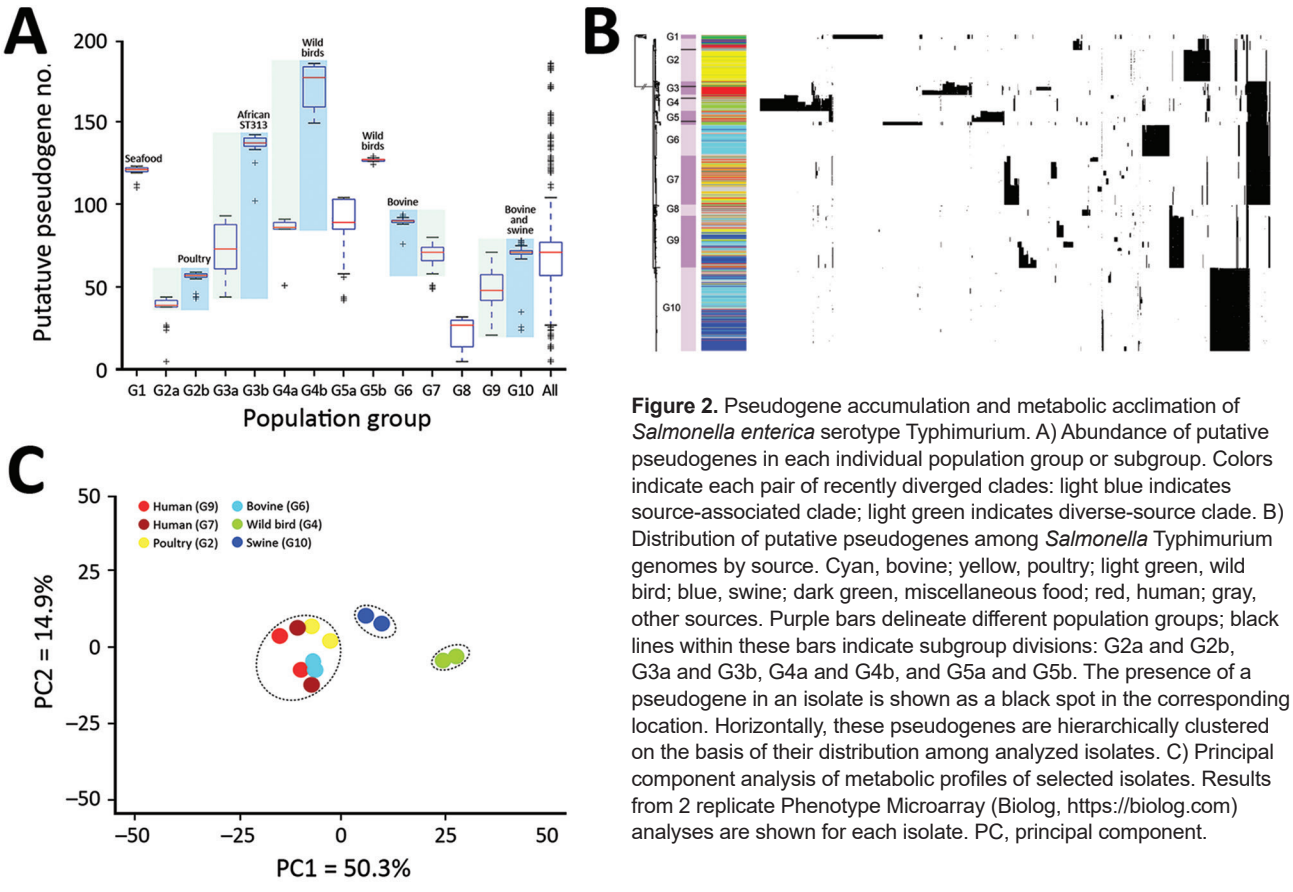

Figure 2. Pseudogene accumulation and metabolic acclimation of *Salmonella enterica* serotype Typhimurium. A) Abundance of putative pseudogenes in each individual population group or subgroup. Colors indicate each pair of recently diverged clades: light blue indicates source-associated clade; light green indicates diverse-source clade. B) Distribution of putative pseudogenes among *Salmonella* Typhimurium genomes by source. Cyan, bovine; yellow, poultry; light green, wild bird; blue, swine; dark green, miscellaneous food; red, human; gray, other sources. Purple bars delineate different population groups; black lines within these bars indicate subgroup divisions: G2a and G2b, G3a and G3b, G4a and G4b, and G5a and G5b. The presence of a pseudogene in an isolate is shown as a black spot in the corresponding location. Horizontally, these pseudogenes are hierarchically clustered on the basis of their distribution among analyzed isolates. C) Principal component analysis of metabolic profiles of selected isolates. Results from 2 replicate Phenotype Microarray (Biolog, https://biolog.com) analyses are shown for each isolate. PC, principal component.

led to 8 zoonotic outbreaks for retrospective source attribution; and 3) excluding 744 redundant genomes to minimize biases resulting from repeated sampling of closely related strains. The genome updates resulted in a modified collection of 1,473 isolates for source prediction, all belonging to the previously defined 10 populations groups.

We observed phylogenetic clustering of isolates from the same zoonotic source (Figure 1, panel A). In general, 70.3% of isolates from bovine, poultry, swine, or wild bird (BPSW) sources shared the MRCA with an isolate from the same source, suggesting the possibility of source prediction by phylogenetic placement. By assigning a query outbreak isolate to the source of the livestock isolate that shared the MRCA with the query, we correctly predicted zoonotic sources for 6 of the 8 zoonotic outbreaks. Most of the reference isolates for source prediction were epidemiologically unrelated to the query isolates (i.e., separated by years [Table 1]). By contrast, only 36.9% of human isolates and 45.5% of food isolates (excluding G1) were from the same source as their nearest phylogenetic neighbor.

In addition to overall phylogeny, we evaluated how the assortment of certain genetic features into particular *Salmonella* Typhimurium genomes could help predict zoonotic sources of *Salmonella* Typhimurium. Using a machine learning approach, we built a Random Forest (RF) classifier to interrogate a comprehensive collection of 3,137 genetic features among *Salmonella* Typhimurium genomes: core genome SNPs (n = 1,882), high-quality insertion/deletions (indels; n = 150), and source discriminatory accessory genes (n = 1,105). Trained by genomes of known BPSW origins, the classifier produced an out-of-bag accuracy rate (https://www.stat.berkeley.edu/~breiman/OOBestimation.pdf) of 82.9%. Seven of the 8 zoonotic outbreaks were attributed to the correct source by the RF method (Table 1).

Among BPSW, the classifier performed best in predicting poultry and swine sources, followed by bovine and wild bird sources (Figure 3, panel A). This result was consistent with relative sampling intensities of these sources. Rarefaction analysis suggested that phylogenetic diversity was better sampled for poultry and swine than bovine and wild bird sources; wild bird *Salmonella* Typhimurium populations were least sampled (Appendix 2 section 9). For each isolate analyzed, the RF classifier generated a predicted probability for each source class. Because the classifier was not trained by isolates from non-BPSW sources, source prediction ambiguities

Table 1. Retrospective source attribution of zoonotic outbreaks of *Salmonella enterica* serotype Typhimurium, United States*

	Outbreak		Phylogenetic reference†			Population	Phylogeny	RF
Isolate	Year	Confirmed vehicle	Isolate	Year	Source	group	prediction	prediction
STM2207	2013	Ground beef	STM296	2006	Bovine	G9	+	+
STM2208	2013	Ground beef	STM296	2006	Bovine	G9	+	+
STM2209	2007	Pot pie turkey	STM093	2005	Poultry	G7	+	+
STM2210	2007	Pot pie turkey	STM093	2005	Poultry	G7	+	+
STM2211	2007	Pot pie turkey	STM093	2005	Poultry	G7	+	+
STM2212	2007	Pot pie turkey	STM093	2005	Poultry	G7	+	+
STM2213	2013	Live poultry	STM2114	2016	Bovine	G7	–	+
STM2214	2013	Live poultry	STM2114	2016	Bovine	G7	–	+
STM2215	2011	Ground beef	STM1563	2011	Bovine	G6	+	+
STM2216	2011	Ground beef	STM1563	2011	Bovine	G6	+	+
STM2217	2015	Pork	STM2116	2016	Swine	G2a	+	+
STM1016	2010	Cattle contact	STM328	2008	Bovine	G9	+	+
STM1075	2010	Cattle contact	STM978	2010	Bovine	G2a	+	+
STM995	2010	Cattle contact	STM978	2010	Bovine	G2a	+	–
STM996	2010	Cattle contact	STM978	2010	Bovine	G2a	+	–
STM1065	1998	Raw milk	STM034	2004	Bovine	G9	+	+
STM988	2009	Chicken	STM1975	2015	Bovine	G9	–	+

*RF, Random Forest; +, correct prediction; –, incorrect prediction.
†The livestock genome that had the most recent common ancestor with an outbreak query genome.

were anticipated when it was used to predict non-BPSW isolates. Such ambiguities might present themselves as increased uncertainty in source prediction. We used the Simpson diversity indices (SDI) to measure the uncertainty of predicted probabilities between BPSW and non-BPSW isolates. The SDI of the non-BPSW group was significantly higher ($p<0.01$) than that of the BPSW group (Figure 3, panel B). We further showed that SDI of predicted probabilities made an effective binary classifier to distinguish BPSW from non-BPSW isolates in the current dataset through a receiver operating characteristic analysis, which yielded a sensitivity of 0.80 and a specificity of 0.63 adopting an arbitrary SDI cutoff of 0.45 (Figure 3, panel C).

Using this cutoff, we categorized source predictions into precise and imprecise groups (Figure 3, panel D). Precise predictions (SDI <0.45) were generated for 829 of 1,041 BPSW isolates, of which 759 (91.6%) were correct. A total of 147 non-BPSW isolates were precisely attributed to a BPSW source; among these, 51 were human isolates, which accounted for 31.9% of human isolates in the *Salmonella* Typhimurium collection.

Zoonotic source predictions by phylogenetic placement and RF analysis were generally consistent (Appendix 1 Table 6). Among the 829 isolates with precise predictions by the RF classifier, 705 (85.0%) isolates were correctly predicted by both methods. Detailed comparison of the 2 methods can be found in Appendix 2 section 10.

Genetic Indicators of Source Association

Using RF, we ranked all 3,137 genetic features by their importance for source prediction, which was measured by the mean decrease of prediction accuracy through randomly permuting feature values (Appendix 1 Table 7). To identify a subset of key features for source prediction, we incrementally incorporated features into the classifier based on their importance ranking and monitored the change of out-of-bag error rate. After an initial sharp drop, the error rate plateaued when ≈50 top-ranking features were included (Figure 4, panel A). Ten core genome mutations were among the top 50 features, 3 nonsynonymous SNPs and 7 indels (Figure 4, panel B). The 2 most important features for source prediction were nonsynonymous SNPs and related to cell surface components (Table 2). One of these was in the *fliC* gene, which is responsible for *Salmonella* flagellum formation and serotype determination. Forty of the other top 50 features were accessory genes found on plasmid- or phage-associated sequences (Figure 4, panel B). Several of these genes were involved in *Salmonella* interaction with host and environment, such as virulence genes *spvB* (*23*), *spvD* (*22*), and *pipB2* (*20*); virulence and putative host range factor *sspH2* (*19*); and multiple resistance genes to silver and copper (Table 2). Both elements are used as dietary supplements or antimicrobial drugs in livestock production (*24*,*25*). Another highly ranked accessory gene, *proQ*, was recently discovered to mediate global posttranscriptional regulation of gene expression (*21*). Twenty-four of the top 50 feature-related genes had been functionally tested for mediating intestinal colonization of livestock animals; 14 showed positive evidence for such a role (*9*). Although not ranked among the top 50 features, antimicrobial resistance genes exhibited enrichment and source-associated distribution patterns among livestock clades (Appendix 2 section 12).

Discussion

Based on our determination of the large-scale phylogeny of *Salmonella* Typhimurium, including dense sampling of US livestock isolates, we speculate emerging host adaptation associated with livestock production. Evidence to

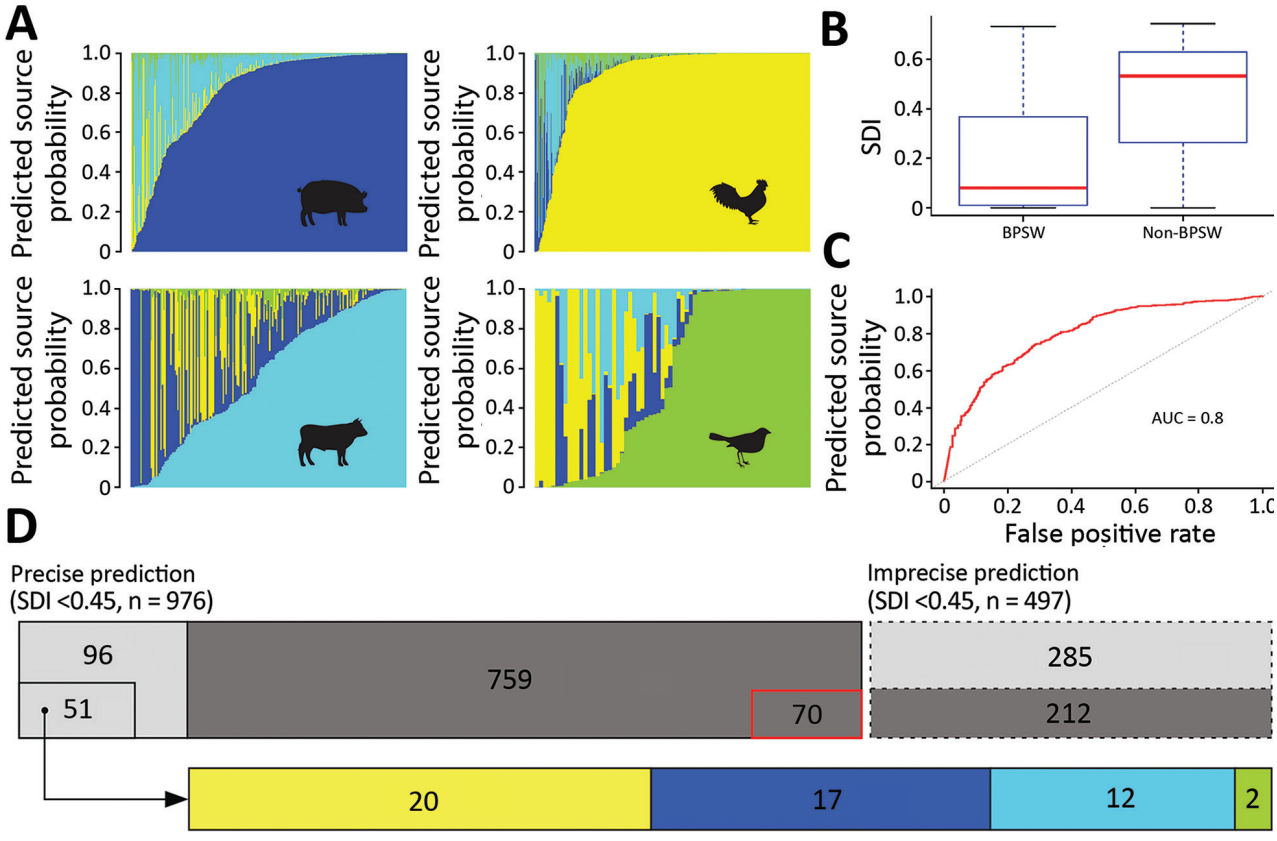

Figure 3. Source prediction by Random Forest classifier. A) Predicted source probabilities for zoonotic *Salmonella enterica* serotype Typhimurium isolates. Each vertical line in a panel is color coded by predicted source probabilities to proportion: cyan, bovine; yellow, poultry; blue, swine; light green, wild bird. B) Comparison of SDIs of predicted probabilities between BPSW and non-BPSW isolates. For each isolate, SDI was calculated among predicted probabilities of the 4 sources. Red horizontal lines indicate median SDI values; blue box tops and bottoms indicate interquartile ranges; whiskers indicate maximum and minimum SDI values. C) Receiver operating characteristics (ROC) curve of differentiating BPSW and non-BPSW isolates using SDI of predicted source probabilities. The AUC was 0.8, suggesting good binary classification. Red line indicates ROC curve; dotted line indicates diagonal line across the ROC space. D) Summary of source prediction results of 1,473 *Salmonella* Typhimurium isolates. Rectangles with solid and dashed lines represent precise (SDI <0.45) and imprecise (SDI >0.45) predictions, respectively. Dark gray rectangles, BPSW isolates; light gray rectangles, non-BPSW isolates. The number in each enclosed area is the number of isolates in the category. The sizes of enclosed and gray areas are in proportion to the numbers of isolates they represent. Red lines highlight the 70 precisely but incorrectly predicted BPSW isolates are shown with red shading. The 51 precisely predicted human isolates were attributed to zoonotic sources: cyan, bovine; yellow, poultry; blue, swine; light green, wild bird. The sizes of source colored rectangles are proportional to the numbers of isolates in the predicted source classes. AUC, area under the ROC curve; BPSW, bovine, poultry, swine, or wild bird; SDI, Simpson diversity index.

support this hypothesis includes increasing pseudogene accumulation as livestock clades diverged and metabolic deviation of a representative swine isolate. Both phenomena have been reported as possible signs of *Salmonella* host adaptation (*26*–*29*). These adaptation signals were detectable but moderate compared with the wild bird and ST313 clades, indicating emerging adaptation. Major clades of livestock isolates (G2b, G6, and G10) occupied terminal branches of the phylogeny and shared recent common ancestors with diverse-source clades, suggesting their recent emergence through clonal expansion. An exhaustive screening for temporal signals throughout the phylogeny enabled MRCA dating of 2 livestock clades in G2b and G10 around the 1990s, supporting their recent origin. The G10 clade contained the swine isolate displaying putative metabolic acclimation, as well as definitive type 104 isolates (Figure 1, panel B), whose global circulation started around the 1990s (*5*), consistent with our MRCA dating.

Major livestock clades all included animal isolates across the United States and spanned >10 years. Phylogenetic clustering of isolates spanning a wide geotemporal range also has been noticed in poultry-related *Salmonella* Enteritidis in the United States (*30*). The dissemination of

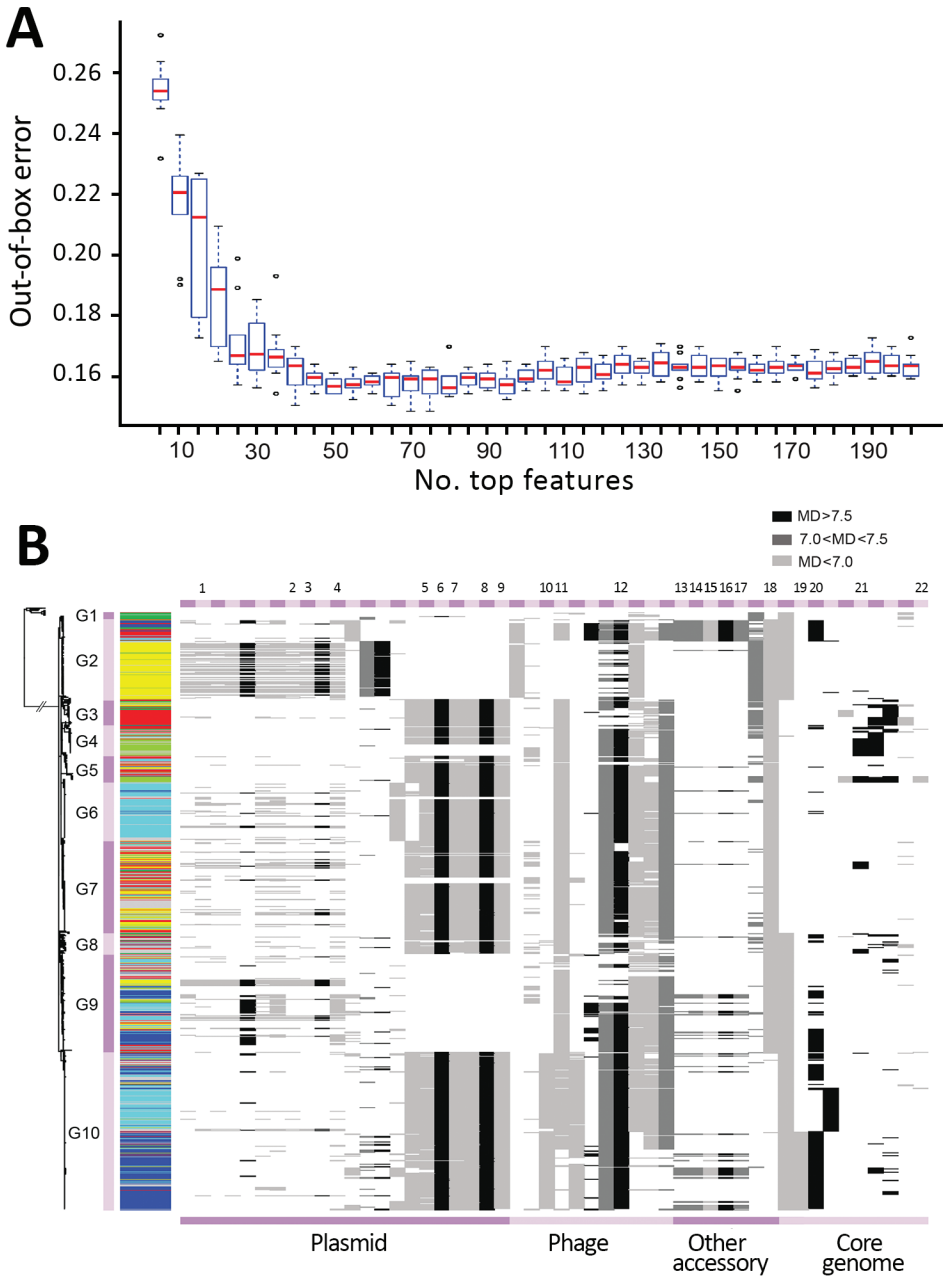

Figure 4. Key genetic features for zoonotic source prediction of *Salmonella enterica* serotype Typhimurium using Random Forest classifier. A) Change of out-of-bag prediction error rate as incremental inclusion of top ranking genetic features for source prediction. Red lines indicate median values; blue boxes indicate interquartile ranges. Upper and lower whiskers indicate maximum and minimum values. Circles indicate outliers. B) Distribution of top 50 source predicting features among *Salmonella* Typhimurium isolates on the basis of their location. Cyan, bovine; yellow, poultry; light green, wild bird; blue, swine; dark green, miscellaneous food; red, human; gray, other sources. Numbers at top reference genes: 1. *proQ*; 2. *exc*; 3. *yafA*; 4.*yceA*; 5. *Trap*; 6. *traA*; 7. *traJ*; 8. *spvB*; 9. *spvD*; 10. *pipB2*; 11. *sspH2*; 12. 1930; 13. *cusA*; 14. *siiP*; 15. *cusC*; 16. *cusF*; 17. *cusB*; 18. 0286A; 19.0835; 20. *fiiC*; 21. 1874; 22. *yhfL*. The presence of a feature in an isolate is shown as a horizontal line in the corresponding location, with its grayscale representing the level of the MD of prediction accuracy through randomly permuting values of the feature. The higher the MD, the more important the feature is for source prediction. MD, mean decrease.

closely related *Salmonella* strains from specific sources in the poultry sector could explain these observations.

Host prediction of *Salmonella* and *Escherichia coli* genomes through a machine-learning approach has been recently reported (*31*,*32*). A machine-learning classifier is inherently constrained by the representativeness of its training classes. However, for application in a realistic source attribution scenario, a classifier would be applied prospectively to isolates from sources a priori unknown to the classifier. Unlike those used in previous studies, our RF classifier was tested by isolates from various nontraining sources and capable of flagging them as imprecise predictions. This distinction might be useful for analyzing foodborne pathogens of a wide source range.

A previous support vector machine classifier had >90% accuracy in predicting the human host of *Salmonella* Typhimurium isolates using WGS data (*32*). Although human is not a source category in foodborne pathogen source attribution studies, which aim to attribute known human isolates to food and other sources, we performed a similar host specificity prediction using our RF classifier and *Salmonella* Typhimurium dataset. Only 36.9% of human isolates in our study were predicted to originate

Table 2. Selected key genetic features for zoonotic source prediction of *Salmonella enterica* serotype Typhimurium using a Random Forest classifier

Feature rank*	Affected gene	Feature type	Gene function (reference)
1	*fliC*	Single-nucleotide polymorphism	Motility, serotype diversity, intestinal colonization (*16*)
5	*traA*	Accessory gene	Pilin precursor. intestinal colonization (*16*)
6	*spvB*	Accessory gene	Virulence (*17*), intestinal colonization (*16*)
9	1930†	Accessory gene	Intestinal colonization (*16*)
11	1874†	Indel	Intestinal colonization (*16*)
13–15, 28	*cusCFBA*	Accessory gene	Putative copper efflux system (*18*)
16	*silP*	Accessory gene	Silver efflux pump (*17*)
21	*yafA*	Accessory gene	Intestinal colonization (*16*)
24	*sspH2*	Accessory gene	Virulence and potential host range factor (*19*)
27	0286A†	Accessory gene	Intestinal colonization (*16*)
31	*pipB2*	Accessory gene	Virulence (*20*)
32	*proQ*	Accessory gene	Global posttranscription regulation (*21*), intestinal colonization (*16*)
34	*spvD*	Accessory gene	Virulence (*22*)
37	*Trap*	Accessory gene	Intestinal colonization (*16*)
39	*yhfL*	Indel	Intestinal colonization (*16*)
41	0835†	Accessory gene	Intestinal colonization (*16*)
43	*traJ*	Accessory gene	Intestinal colonization (*16*)
45	*yceA*	Accessory gene	Intestinal colonization (*16*)
46	*exc*	Accessory gene	Intestinal colonization (*16*)

*Features are ranked by the mean decrease of prediction accuracy through randomly permuting values of the feature. The larger the mean decrease, the higher the rank. Only features that are located in genes that have reported involvement in intestinal colonization, virulence, and other functions related to livestock environment adaptation are listed. The full list of analyzed features, including the top 50 for zoonotic source prediction, is provided in Appendix 1 Table 6 (https://wwwnc.cdc.gov/EID/article/25/1/18-0835-App1.xlsx). Indel, insertion/deletion.
†Locus identification of the reference genome SL1344.

from a human host (Appendix 2 section 11). We found that the higher accuracy of human host prediction by the support vector machine classifier (*32*) was due mainly to an exceedingly clonal structure of its training human isolates, of which 85% shared the MRCA with another human isolate, compared with only 36.9% in our training set (Appendix 2 section 13). The percentage for the training set was consistent with our sampling of diverse human isolates in the United States based on surveillance data, including molecular subtypes. To avoid inflating source prediction accuracy by overrepresenting closely related genomes in the training set, we reduced training data redundancy by excluding 744 genomes from all training classes based on their pairwise phylogenetic distance and strain metadata (Appendix 2 section 6). Our classifier could not distinguish US human isolates from isolates of other sources by genomewide analysis of genetic features, arguing against distinct human host signals in *Salmonella* Typhimurium genomes or suggesting that the human isolates represent a mixture of strains immediately derived from multiple other sources. Higher occurrence of certain *Salmonella* Typhimurium subtypes in human cases, therefore, more likely results from their prevalent circulation in foods and the environment, as observed in G7, than from elevated infectivity or virulence.

The known zoonotic hosts and reservoirs of *Salmonella* Typhimurium appeared to be highly attributable. When the classifier was precise about a BPSW origin, 91.6% of isolates were correctly predicted. A narrow coverage of livestock isolate diversity in the United States could skew prediction accuracy. This scenario was countered by the inclusion of isolates from major US *Salmonella* Typhimurium outbreaks of livestock origins over 15 years, most of which our classifier correctly predicted. Furthermore, livestock populations of *Salmonella* Typhimurium appeared to be more clonal than human isolates (Figure 1, panel A), possibly in association with industrialized livestock production.

Our classifier performed genomewide, high-resolution interrogations of genetic features, including not only accessory genes as previously reported (*31*,*32*) but also core genome mutations, such as SNPs and indels. This approach led to the discovery of a point mutation in *fliC* that outperformed all the other features in source prediction. *fliC* encodes the filament portion of the bacterial flagella, flagellin. Flagellin shows substantial antigenic diversity across *Salmonella* that has been exploited for *Salmonella* serotyping. It remains unclear whether the 2 different FliC proteins we discovered have different biologic properties that might correlate to zoonotic source. Our demonstration that a few key genetic features were sufficient for robust source prediction paves the way for developing efficient source attribution models scalable to large and expanding volumes of WGS data, which in turn is likely to improve the training and performance of the RF classifier.

Our classifier and pilot source attribution study based on the current training set is limited to predicting major livestock sources of *Salmonella* Typhimurium. Fewer than one third (31.9%) of human isolates were precisely attributed to a BPSW source, indicating additional sources of human salmonellosis underrepresented

by the current training set. Continuing accumulation of *Salmonella* Typhimurium genomes from environmental sources might be expected to lead to the identification of additional source classes to enable source attribution of more human clinical isolates using the machine-learning approach and could potentially help generate source hypotheses for outbreak investigation. Regular update of the training set is required for incremental improvement of the classifier, particularly for tracking new and emerging strains.

Another limitation is related to the ability of certain *Salmonella* Typhimurium isolates to circulate among multiple sources, which challenges precise source prediction. For example, source prediction of BPSW isolates in the diverse-source G7 lineage was lower at 64.2% than the out-of-bag prediction accuracy at 82.9% of all BPSW isolates. Nevertheless, G7 isolates from the 2009 turkey pot pie–associated outbreak and the 2013 live poultry–associated outbreak were attributed to poultry. These successful attributions were most likely due to the inclusion of other G7 poultry isolates in the training set that informed the classifier. Growing availability of training genomes in generalist lineages may reveal fine-scale clustering of *Salmonella* Typhimurium isolates by source to help source prediction.

Finally, transmission of *Salmonella* from a zoonotic source to a nonanimal food vehicle is possible. For example, domesticated and wild animals can cause *Salmonella* contamination of irrigation water, which may subsequently contaminate fresh produce (*33*). Two G7 outbreaks with precise source predictions were linked to fresh produce, the 2010–2011 multistate alfalfa sprout–associated outbreak and the 2012 multistate cantaloupe-associated outbreak. In both cases, the outbreak isolates were attributed to poultry. Although the findings cannot be confirmed, our study provides a potential new tool to help identify root sources of foodborne *Salmonella* Typhimurium outbreaks.

Acknowledgments

We are grateful to Nadejda Lupolova and David Gally for sharing *Salmonella* genomes from their study.

About the Author

Dr. Zhang is a postdoctoral fellow at the Center for Food Safety, University of Georgia. His primary research interests include bioinformatics and genomic epidemiology of *Salmonella*.

References

1. Scallan E, Hoekstra RM, Angulo FJ, Tauxe RV, Widdowson MA, Roy SL, et al. Foodborne illness acquired in the United States—major pathogens. Emerg Infect Dis. 2011;17:7–15. http://dx.doi.org/10.3201/eid1701.P11101
2. Hoffmann S, Maculloch B, Batz M. Economic burden of major foodborne illnesses acquired in the United States [cited 2018 Oct 8]. https://www.ers.usda.gov/webdocs/publications/43984/52807_eib140.pdf
3. Hendriksen RS, Vieira AR, Karlsmose S, Lo Fo Wong DM, Jensen AB, Wegener HC, et al. Global monitoring of *Salmonella* serovar distribution from the World Health Organization Global Foodborne Infections Network Country Data Bank: results of quality assured laboratories from 2001 to 2007. Foodborne Pathog Dis. 2011;8:887–900. http://dx.doi.org/10.1089/fpd.2010.0787
4. Rabsch W, Andrews HL, Kingsley RA, Prager R, Tschäpe H, Adams LG, et al. *Salmonella enterica* serotype Typhimurium and its host-adapted variants. Infect Immun. 2002;70:2249–55. http://dx.doi.org/10.1128/IAI.70.5.2249-2255.2002
5. Helms M, Ethelberg S, Mølbak K; DT104 Study Group. International *Salmonella* Typhimurium DT104 infections, 1992–2001. Emerg Infect Dis. 2005;11:859–67. http://dx.doi.org/10.3201/eid1106.041017
6. Okoro CK, Kingsley RA, Connor TR, Harris SR, Parry CM, Al-Mashhadani MN, et al. Intracontinental spread of human invasive *Salmonella* Typhimurium pathovariants in sub-Saharan Africa. Nat Genet. 2012;44:1215–21. http://dx.doi.org/10.1038/ng.2423
7. Graham SM. Nontyphoidal salmonellosis in Africa. Curr Opin Infect Dis. 2010;23:409–14. http://dx.doi.org/10.1097/QCO.0b013e32833dd25d
8. Yue M, Han X, De Masi L, Zhu C, Ma X, Zhang J, et al. Allelic variation contributes to bacterial host specificity. Nat Commun. 2015;6:8754. http://dx.doi.org/10.1038/ncomms9754
9. Chaudhuri RR, Morgan E, Peters SE, Pleasance SJ, Hudson DL, Davies HM, et al. Comprehensive assignment of roles for *Salmonella* Typhimurium genes in intestinal colonization of food-producing animals. PLoS Genet. 2013;9:e1003456. http://dx.doi.org/10.1371/journal.pgen.1003456
10. Pires SM, Evers EG, van Pelt W, Ayers T, Scallan E, Angulo FJ, et al.; Med-Vet-Net Workpackage 28 Working Group. Attributing the human disease burden of foodborne infections to specific sources. Foodborne Pathog Dis. 2009;6:417–24. http://dx.doi.org/10.1089/fpd.2008.0208
11. Hald T, Vose D, Wegener HC, Koupeev T. A Bayesian approach to quantify the contribution of animal-food sources to human salmonellosis. Risk Anal. 2004;24:255–69. http://dx.doi.org/10.1111/j.0272-4332.2004.00427.x
12. Barco L, Barrucci F, Olsen JE, Ricci A. *Salmonella* source attribution based on microbial subtyping. Int J Food Microbiol. 2013;163:193–203. http://dx.doi.org/10.1016/j.ijfoodmicro.2013.03.005
13. Swaminathan B, Barrett TJ, Hunter SB, Tauxe RV; CDC PulseNet Task Force. PulseNet: the molecular subtyping network for foodborne bacterial disease surveillance, United States. Emerg Infect Dis. 2001;7:382–9. http://dx.doi.org/10.3201/eid0703.017303
14. Allard MW, Strain E, Melka D, Bunning K, Musser SM, Brown EW, et al. Practical value of food pathogen traceability through building a whole-genome sequencing network and database. J Clin Microbiol. 2016;54:1975–83. http://dx.doi.org/10.1128/JCM.00081-16
15. Zhang S, Yin Y, Jones MB, Zhang Z, Deatherage Kaiser BL, Dinsmore BA, et al. *Salmonella* serotype determination utilizing high-throughput genome sequencing data. J Clin Microbiol. 2015;53:1685–92. http://dx.doi.org/10.1128/JCM.00323-15
16. Chaudhuri RR, Morgan E, Peters SE, Pleasance SJ, Hudson DL, Davies HM, et al. Comprehensive assignment of roles for *Salmonella* typhimurium genes in intestinal colonization of food-producing animals. PLoS Genet. 2013;9:e1003456. http://dx.doi.org/10.1371/journal.pgen.1003456

17. Gupta A, Matsui K, Lo JF, Silver S. Molecular basis for resistance to silver cations in *Salmonella.* Nat Med. 1999;5:183–8. http://dx.doi.org/10.1038/5545
18. Franke S, Grass G, Rensing C, Nies DH. Molecular analysis of the copper-transporting efflux system CusCFBA of *Escherichia coli.* J Bacteriol. 2003;185:3804–12. http://dx.doi.org/10.1128/JB.185.13.3804-3812.2003
19. Tsolis RM, Townsend SM, Miao EA, Miller SI, Ficht TA, Adams LG, et al. Identification of a putative *Salmonella enterica* serotype typhimurium host range factor with homology to IpaH and YopM by signature-tagged mutagenesis. Infect Immun. 1999;67:6385–93.
20. Henry T, Couillault C, Rockenfeller P, Boucrot E, Dumont A, Schroeder N, et al. The *Salmonella* effector protein PipB2 is a linker for kinesin-1. Proc Natl Acad Sci U S A. 2006;103:13497–502. http://dx.doi.org/10.1073/pnas.0605443103
21. Smirnov A, Förstner KU, Holmqvist E, Otto A, Günster R, Becher D, et al. Grad-seq guides the discovery of ProQ as a major small RNA-binding protein. Proc Natl Acad Sci U S A. 2016;113:11591–6. http://dx.doi.org/10.1073/pnas.1609981113
22. Grabe GJ, Zhang Y, Przydacz M, Rolhion N, Yang Y, Pruneda JN, et al. The *Salmonella* effector SpvD Is a cysteine hydrolase with a serovar-specific polymorphism influencing catalytic activity, suppression of immune responses, and bacterial virulence. J Biol Chem. 2016;291:25853–63. http://dx.doi.org/10.1074/jbc.M116.752782
23. Lesnick ML, Reiner NE, Fierer J, Guiney DG. The *Salmonella* spvB virulence gene encodes an enzyme that ADP-ribosylates actin and destabilizes the cytoskeleton of eukaryotic cells. Mol Microbiol. 2001;39:1464–70. http://dx.doi.org/10.1046/j.1365-2958.2001.02360.x
24. Yazdankhah S, Rudi K, Bernhoft A. Zinc and copper in animal feed—development of resistance and co-resistance to antimicrobial agents in bacteria of animal origin. Microb Ecol Health Dis. 2014; 25:25.
25. Gupta A, Silver S. Silver as a biocide: will resistance become a problem? Nat Biotechnol. 1998;16:888. http://dx.doi.org/10.1038/nbt1098-888
26. Thomson NR, Clayton DJ, Windhorst D, Vernikos G, Davidson S, Churcher C, et al. Comparative genome analysis of *Salmonella* Enteritidis PT4 and *Salmonella* Gallinarum 287/91 provides insights into evolutionary and host adaptation pathways. Genome Res. 2008;18:1624–37. http://dx.doi.org/10.1101/gr.077404.108
27. Holt KE, Thomson NR, Wain J, Langridge GC, Hasan R, Bhutta ZA, et al. Pseudogene accumulation in the evolutionary histories of *Salmonella enterica* serovars Paratyphi A and Typhi. BMC Genomics. 2009;10:36. http://dx.doi.org/10.1186/1471-2164-10-36
28. Langridge GC, Fookes M, Connor TR, Feltwell T, Feasey N, Parsons BN, et al. Patterns of genome evolution that have accompanied host adaptation in *Salmonella.* Proc Natl Acad Sci U S A. 2015;112:863–8. http://dx.doi.org/10.1073/pnas.1416707112
29. Feasey NA, Hadfield J, Keddy KH, Dallman TJ, Jacobs J, Deng X, et al. Distinct *Salmonella* Enteritidis lineages associated with enterocolitis in high-income settings and invasive disease in low-income settings. Nat Genet. 2016;48:1211–7.http://dx.doi.org/10.1038/ng.3644
30. Deng X, Desai PT, den Bakker HC, Mikoleit M, Tolar B, Trees E, et al. Genomic epidemiology of *Salmonella enterica* serotype Enteritidis based on population structure of prevalent lineages. Emerg Infect Dis. 2014;20:1481–9. http://dx.doi.org/10.3201/eid2009.131095
31. Lupolova N, Dallman TJ, Matthews L, Bono JL, Gally DL. Support vector machine applied to predict the zoonotic potential of *E. coli* O157 cattle isolates. Proc Natl Acad Sci U S A. 2016;113:11312–7. http://dx.doi.org/10.1073/pnas.1606567113
32. Lupolova N, Dallman TJ, Holden NJ, Gally DL. Patchy promiscuity: machine learning applied to predict the host specificity of *Salmonella enterica* and *Escherichia coli.* Microb Genom. 2017;3:e000135. http://dx.doi.org/10.1099/mgen.0.000135
33. Hanning IB, Nutt JD, Ricke SC. Salmonellosis outbreaks in the United States due to fresh produce: sources and potential intervention measures. Foodborne Pathog Dis. 2009;6:635–48. http://dx.doi.org/10.1089/fpd.2008.0232

Address for correspondence: Xiangyu Deng, University of Georgia, Center for Food Safety, 1109 Experiment St, Griffin, GA 30223, USA; email: xdeng@uga.edu

Article DOI: https://doi.org/10.3201/eid2501.180835

Zoonotic Source Attribution of *Salmonella enterica* Serotype Typhimurium Using Genomic Surveillance Data, United States

Appendix 2

1. Sequencing and Selection of *Salmonella enterica* serotype Typhimurium Genomes

A total of 127 human clinical isolates were grown in tryptic soy broth (TSB) overnight. Genomic DNA was extracted by using the GenElute Genomic DNA isolation kit (Sigma-Aldrich, St. Louis, MO, USA). Sequencing libraries were prepared using Illumina TruSeq DNA library kit (San Diego, CA, USA) and sequenced on an Illumina HiSeq instrument (San Diego, CA, USA) according to manufacturer's instruction. Trimmomatic v0.32 (*1*) was used to remove low-quality reads. The leading 3 and the trailing 3 nucleotides were removed from the reads, and a 4-nucleotide sliding window was used to remove nucleotides from the 3′ ends when the average Phred score dropped below 20. Then the raw reads were assembled into draft genomes using SPAdes v3.7.0 by default settings (*2*). The quality of publicly available *S. enterica* Typhimurium draft genomes used in this study was assessed by QUAST v4.5 (*3*). Assemblies with an N50 value <100,000 were excluded from further analysis.

2. Phylogenetic Analysis

Genome regions related to repetitive sequences, phages, and recombination were removed from the reference genome prior to phylogeny construction. Repetitive and phage sequences were detected in the reference SL1344 genome (NCBI accession: NC_016810) by MUMmer v3.23 (*4*) and Phast (*5*), respectively. Recombinant sequences were identified by taking the union of the inferences by Gubbins v2.2.0 (*6*) and ClonalFrameML v1.25 (*7*). Genomes in the G1 group were excluded from recombination analysis because their phylogenetic distance with the rest of *S. enterica* Typhimurium genomes was too distant for the recombination

detection tools to properly detect recombination. Draft genomes were assembled from raw sequencing reads using SPAdes (*2*). A maximum-likelihood phylogenetic tree was constructed by FastTree2 v2.1.7 (*8*) based on core genome alignment of draft and finished *S. enterica* Typhimurium genomes through Parsnp v1.2 (*9*). The modified SL1344 genome free of inferred repetitive, phage, and recombinant sequences was used as a reference for the alignment. Major population groups were identified using BAPS v6.0 (*10*). Two levels with a maximum 50 populations were set as the initial condition for BAPS to infer population structure of *S. enterica* Typhimurium genomes using a maximum-likelihood approach.

3. Temporal Signal Identification and MRCA Dating

To preliminarily explore local temporal signals of SNP accumulation throughout the global phylogeny of *S. enterica* Typhimurium, every subtree (i.e. internal node) of the phylogeny was screened by calculating the Spearman's correlation coefficient and the Pearson's correlation coefficient between isolation years of the corresponding isolates and tip-to-root (i.e., the internal node) distances of these isolates. We used both Spearman's and Pearson's correlation coefficients as preliminary screening metrics to maximize the discovery of candidate subtrees displaying temporal signals of SNP accumulation. Subtrees whose squared coefficient (R2) of either the Spearman's or the Pearson's correlation exceeded 0.4 were selected for further temporal analysis. Pearson's correlation was used as a secondary screening metric; if an internal node had a R2 over 0.4 for Spearman's, Pearson's correlation was not calculated. Raw reads of genomes in each candidate subtree were first aligned to their nearest finished genome on the global phylogeny using BWA v0.7.12 (*11*). The use of a closely related reference genome when available maximized the detection of SNPs present among the members of a subtree, but absent from a more distant reference genome. High quality SNPs were called using FreeBayes v1.1.0-44 (*12*). These SNPs were defined to meet 3 criteria: 1) a minimum of 5 reads were mapped to the SNP locus, 2) at least 75% of mapped reads supported the SNP calling, and 3) a minimum mapping quality score generated by BWA at the SNP locus was 20. Concatenated high quality SNPs were used to construct a maximum-likelihood tree by Phyml v20120412 (*13*). Then, TempEst v1.5 (*14*) was used to repeat the calculation of the linear coefficient between isolation years and branch lengths of candidate subtrees to confirm their temporal signals. Any subtree with R2 >0.4 was considered to display a temporal signal and then subjected to model-based

population dynamics analysis using BEAST v1.8.2 (*15*) with at least 200,000,000 states and sampling of every 5,000. The maximum clade credibility tree was generated by TreeAnnotator v1.8.2 (http://beast.bio.ed.ac.uk/TreeAnnotator) to estimate the ages of most recent common ancestors. Model performance was assessed through Tracer v1.6 (http://beast.bio.ed.ac.uk/Tracer). Four different combinations of tree and clock models were tested for each clade and compared through Bayes factors (BF) (*16*): 1) Gaussian Markov Random Fields (GMRF) as tree model and relaxed log-normal molecular clock as clock model, 2) GMRF as tree model and strict clock rate as clock model, 3) constant population model as tree model and relaxed log-normal molecular clock as clock model, and 4) constant population model as tree model and strict clock rate as clock model. The combination with the highest Bayes factor (BF) was selected for analysis. As shown in Appendix 1 Table 8 (https://wwwnc.cdc.gov/EID/article/25/1/18-0835-App1.xlsx), the combination of Gaussian Markov Random Fields (GMRF) and relaxed log-normal molecular clock was favored for a poultry clade in G2 and a swine clade in G10 by yielding the highest BF among model combinations. For another swine clade in G9, the combination of constant effective population size and relaxed log-normal molecular clock was favored. For all 3 clades, a relaxed log-normal molecular clock was favored over a strict clock rate (log10BF between 17 and 50), suggesting that mutation rates vary among branches. This was consistent with our observation that temporal signal of SNP accumulation was only evident locally in certain clades instead of globally across the entire tree. Estimated substitution rate and most recent common ancestor age for each clade were summarized in Appendix 1 Table 5.

4. Identification of putative pseudogenes

Putative core genome pseudogenes were defined by having any of the following mutations: 1) nonsynonymous SNPs (NS-SNPs) in the start or stop codon; 2) frameshift mutations caused by indels; 3) truncations that spanned at least 20% of a coding region; 4) NS-SNPs or non-frameshift indels that were potentially deleterious (explained below); and 5) premature stop codons. Specifically, indels were identified from raw reads by Scalpel v0.5.3 (*17*) using SL1344 as the reference genome and confirmed by manual inspection. A preliminary indel was first called if 1) a minimum of 5 reads were mapped the locus of the indel, and 2) at least 50% of mapped reads supported the indel calling. High fidelity indels were confirmed through

comparison with corresponding sequences in the reference genome. The reference genome sequence between 100 bp upstream and 100 bp downstream of a preliminary indel was extracted and compared with the draft genome of the *S. enterica* Typhimurium isolate in which the indel was identified. The comparison was performed by BLAST, and the result was manually inspected. Deleterious NS-SNPs were identified by Provean v1.1.5 (*18*). Any NS-SNP with a Provean score lower than a default threshold of –2.5 was considered to be deleterious. To identify gene truncations, the predominant allele of each core gene identified by Roary v3.8.2 (*19*) from de novo assemblies was determined. Any allele with at least 20% of its coding region deleted in comparison with the predominant allele was considered to be truncated. NS-SNPs in start and stop codons and premature stop codons were identified by locating the mutations in the annotated SL1344 reference genome.

When SL1344 (or any genome) is used as the reference to identify mutations in other genomes that may cause putative pseudogenes, it is assumed that alleles in the reference genome represent the wild type, non-mutant forms of the genes. This assumption may not apply to already mutated genes specific to the reference genome. Such reference-specific mutations need to be identified to correct the bias in pseudogene identification caused by the selection of reference genome. NS-SNPs that were present in 1%–99% of the 1,267 *S. enterica* Typhimurium genomes and all of the identified indels were examined for their distribution among the genomes. As shown in Appendix 2 Figure 1, a total of 138 SNPs and 21 indels (highlighted by red dashed box) were found in the majority of population groups, including the distantly related G1 but absent from G5a, in which the reference SL1344 genome was located, and/or a few other population groups that shared a recent common ancestor with G5a. The most parsimonious explanation for this distribution pattern is that these mutations are specific to G5a and its closely related groups, as compared with the less parsimonious hypothesis of multiple independent occurrences of the same mutations in different lineages. Therefore, for pseudogene identification, the SL1344 reference alleles that contained such mutations were replaced by the likely non-mutant alleles inferred from genomes free of these mutations. The final set of putative pseudogenes identified in this study is summarized in Appendix 1 Table 10.

5. Source Classification

Seven source classes were defined for source attribution analysis: 1) human, including human clinical isolates; 2) bovine, including isolates from cattle, beef, and raw milk; 3) poultry, including isolates from chicken, turkey, duck, and eggs; 4) wild birds, including isolates from wild bird species, such as sparrow and gull; 5) swine, including isolates from pigs and pork; 6) miscellaneous food, including seafood such as fish and shrimp, plant-based food such as grains and produce, and other ready-to-eat and/or processed food, such as peanut butter and cheese; and 7) others, including any isolates not belonging to the aforementioned classes. Bovine, poultry, and swine sources were categorized as livestock. Outbreak isolates with confirmed food or livestock origins were assigned to such sources.

6. Random Forest-based Source Attribution

The training set for the RF classifier contained a total of 1,041 genomes from BPSW sources (nbovine = 195, npoultry = 440, nswine = 338 and nwild birds = 68). A total of 2,217 *S. enterica* Typhimurium genomes were collected or sequenced in this study, including the original set of 1,267 genomes by September 2015, an addition of 939 genomes that became publicly available thereafter, and 11 outbreak genomes that were sequenced for retrospective investigation. To alleviate sampling biases due to repetitive inclusion of closely-related isolates, we identified isolates that were separated by a maximum of 10 core genome SNPs and isolated from the same source and in the same geographic location (a US state or a non-US country) and in the same calendar year. One representative was randomly selected from each cluster of closely-related isolates and kept in the study. The rest of the cluster were considered to be redundant and discarded. A total of 744 redundant genomes were removed, leading to a final set of 1,473 genomes for source attribution analysis, including the 1,041 BPSW isolates for classifier training.

To select genetic features for the RF classifier, SNPs, indels and accessory genes were identified from the updated collection of 1,473 non-redundant genomes. SNP, and indel identifications were performed as previously described. Accessory genes were defined as genes present in <99% of the 1,473 genomes. Draft genomes annotated by Prokka v1.12 (*20*) were analyzed by Roary (*19*) to identify accessory genes. A total of 34,892 SNPs, 213 indels, and

29,813 accessory genes were identified. Any SNP and indel that was unique to the non-US G1 group, located in intergenic regions, and present in <1% or >99% of genomes was excluded, leading to the final sets of 1,882 SNPs and 150 indels to be included as genetic features for the RF classifier. Because the sheer number of accessory genes (n = 29,813) was prohibitively large for the RF classifier, accessory genes were further filtered by their source discriminatory power among analyzed *S. enterica* Typhimurium isolates. Specifically, accessory genes unique to the non-US G1 group were excluded first. Then, we defined source prevalence of an accessory gene as the percentage of isolates from a particular source that had the gene. For any accessory gene, if its source prevalence differed by <25% between its most and least prevalent BPSW sources, the gene was considered to be insufficiently discriminatory among sources and removed. After removing these genes, a final set of 1,105 accessory genes were included as genetic features for the RF classifier.

The RF classifier was built using the randomForest package (v4.6-12) of R. The "ntree" argument was set to be 1,000, and default settings were used for other parameters. To estimate prediction errors and infer feature importance, the RF algorithm used out of the bag (OOB) samples created by bootstrap aggregating or bagging of training data (*21*).

7. Elevated Accumulation of Putative Pseudogenes Accompanied the Emergence of Putatively Host-Adapted Clades

Putative pseudogene formation was evident among sub-Saharan ST313 isolates and wild bird isolates. Evidence of host adaptation has been reported for isolates from these sources (*22*,*23*). We examined pseudogene accumulation during the evolutionary emergence of the ST313 clade (G3b) and a wild bird clade (G4b). Putative pseudogenes were identified as described in the Methods section of the main text to include 5 categories of mutations: 1) nonsynonymous SNPs (NS-SNPs) in the start or stop codon; 2) frameshift mutations caused by indels; 3) truncations that spanned at least 20% of a coding region; 4) NS-SNPs or non-frameshift indels that were potentially deleterious; and 5) premature stop codons. The abundance of putative pseudogenes was surveyed in individual clades that shared increasingly more recent common ancestors with the ST313 clade (Appendix 2 Figure 2, panel A) or the wild bird clade (Appendix 2 Figure 2, panel B). The 2 phylogenies shown in Appendix 2 Figure 2 were subtrees

from the entire *S. enterica* Typhimurium tree (Figure 1, panel A) that was mid-point rooted. In both instances, the divergence and evolution of putatively host-adapted lineages appeared to coincide with elevated accumulation of putative pseudogenes. As shown in Appendix 2 Figure 2, more recently diverged clades were associated with higher abundances of putative pseudogenes.

8. Inference of Genotypic Causes of Metabolic Differences

Overall metabolic potentials of 6 representative isolates from 6 major population groups (G2b, G4b, G6, G7, G9, and G10b; Appendix 1 Table 2) were evaluated using Biolog Phenotype Microarrays (PM) (Hayward, CA, USA) according to manufacturer's instruction. Phenotype MicroArray MicroPlates 1-4 (PM1-4) were used for the metabolic profiling. These plates include substrates of carbon (PM1 and PM2), nitrogen (PM3), and sulfur and phosphorus (PM4) sources. The metabolic profiling was performed at 37°C that was similar to body temperatures of humans and other warm-blooded animal hosts of *Salmonella*. Colorimetric measurement of each well was taken every 15 m for 48 h. Data analysis was performed using OmniLog PM System under the default setting. Principal component analysis (PCA) was conducted using the PM results. Among representative isolates from source-associated clades (STM096, STM223, STM481, and STM712), reduced or loss of ability to utilize certain substrates compared with the reference isolate (STM988/2009K-1063) was most evident for a swine isolate (STM712) and a wild bird isolate (STM223) according to the PM analysis (Figure 2, panel C; Appendix 1 Table 2). Their corresponding clades (G10 and G4b) exhibited elevated levels of putative pseudogene accumulation compared with diverse-source clades (Figure 2, panel A). We sought to identify potential genotypic causes for the different metabolic phenotypes. For a substrate that was differentially utilized between the swine/wild bird isolate and the reference isolate, genes involved in corresponding metabolic pathway were identified using KOBAS v3.0 (*24*) and KEGG (*25*). Putative pseudogenes and nonsynonymous SNPs that could potentially disrupt a metabolic pathway were searched in these genes. One example is shown in Appendix 2 Figure 3. It is not clear if the disrupted sulfate reduction pathway plays any role in host adaptation of *S. enterica* Typhimurium. Inferences of genotypic causes of metabolic deviation were summarized in Appendix 1 Table 9.

9. Rarefaction Analysis of Relative Sampling Intensity by Source

A rarefaction analysis was performed to assess relative sampling intensities by sources. Sampling richness was evaluated by measuring the quantity of phylogenetic clusters for each source. A phylogenetic cluster was defined as a monophyletic group of closely related isolates. Individual clusters were delineated by imposing a heuristically determined maximum pairwise SNP distance among isolates within a cluster. This heuristic value determined the sizes as well as the total number of phylogenetic clusters to be identified from the *S. enterica* Typhimurium phylogeny; the lower the value, the more clusters were found. To select a proper value that reflects phylogenetic distance among isolates from source-associated clades, we examined a total of 963 internal nodes from which a minimum of 5 isolates (external nodes) had descended and identified a total of 49 non-overlapping clades associated with bovine, poultry, swine, or wild bird (BPSW). Each of the 49 source-associated clades had at least 75% isolates from the same BPSW source. The maximum pairwise SNP distance in each of these clades was calculated. The mean of these distances was 150 SNPs, which led to the delineation of 205 phylogenetic clusters from the phylogeny of 2,217 genomes. The rarefaction analysis was performed on this dataset using the vegan package v2.4-4 (*26*) in R (*27*). The number of phylogenetic clusters represented by a certain number of isolates was examined for each source (Appendix 2 Figure 4, panel A). The steeper slopes of human and miscellaneous food curves suggested greater diversities were yet to be sampled from human and food isolates than BPSW isolates. The observation of more diverse clusters among human and food isolates also suggested diverse sources of *S. enterica* Typhimurium human infections and food contaminations in addition to BPSW. Less diversity is expected to be uncovered by continuing sampling of BPSW isolates than human and food isolates. Similar trends of relative sampling intensities were observed by adjusting the SNP distance threshold for phylogenetic cluster definition from 150 to 50, 100 and 200 (Appendix 2 Figure 4, panels B–D).

10. Comparison between *S. enterica* Typhimurium Zoonotic Source Predictions Using Phylogenetic Placement and RF Classifier

Among the 829 BPSW isolates that were precisely predicted (Simpson index of predicted source probabilities <0.45), 52 (6.3%) were incorrectly predicted by both RF and phylogenetic

placement (PP), 54 (6.5%) were incorrectly predicted by PP alone, and 18 (2.2%) were incorrectly predicted by RF alone. Source prediction by PP was performed by assigning a query to the source of the livestock isolate that shared the MRCA with the query. A maximum-likelihood phylogeny of *S. enterica* Typhimurium isolates used for source prediction analysis can be viewed at https://itol.embl.de/tree/19813720218255981525121446. An alternative method for source prediction by PP is to identify the predominant source in the clade in which a query isolate is placed and assign the source to the query. This method is algorithmically more complex by requiring arbitrary definitions of clades and source predomination threshold. It is also presumably more sensitive to sampling biases that lead to over- or under-representation of isolates from certain sources and clades, which are commonly found in public depositaries of pathogen genomes.

Incorrect Source Predictions by Both RF and PP (n = 52)

On the phylogenetic tree, nearly all the isolates whose sources were incorrectly predicted by both methods were found in clades that were dominated by isolates from the predicted source. Such cases may be explained by spillover transmissions between different sources. Putative spillover events may have occurred between bovine and swine (n = 20, STM452, STM2167, STM325, STM184, STM027, STM696, STM1173, STM443, STM1661, STM512, STM455, STM471, STM335, STM1359, STM453, STM1620, STM755, STM2004, STM1665, STM1817), poultry and wild bird (n = 10, STM877, STM265, STM224, STM228, STM263, STM257, STM261, STM256, STM258, STM262), swine and poultry (n = 7, STM177, STM1510, STM067, STM1227, STM170, STM1175, STM815), bovine and poultry (n = 1, STM968), bovine and wild birds (n = 1, STM457), and swine and wild birds (n = 2, STM649, STM259). Appendix 2 Figure 5, panel B, shows an example of incorrect prediction caused by a putative spillover infection between wild bird and swine. The isolate involved (STM649) was incorrectly predicted by both methods as wild bird.

A total of 11 genomes (STM433, STM1911, STM266, STM2077, STM294, STM298, STM287, STM260, STM1246, STM166, STM791) for which the source was incorrectly predicted by both methods belonged to clades of diverse sources. These incorrect predictions suggested the challenge for WGS-based source prediction due to likely generalist strains that can be associated with different sources and hosts.

Correct Source Prediction by RF but Incorrect Prediction by PP (n = 54)

Of the 54 isolates whose BPSW sources were correctly predicted by RF but incorrectly predicted by PP, 47 might be attributed to interference caused by putative spillover events that confounded the PP method (STM715, STM704, STM1473, STM754, STM721, STM329, STM327, STM710, STM708, STM1168, STM861, STM727, STM1874, STM1446, STM1952, STM777, STM1986, STM2190, STM2002, STM215, STM204, STM463, STM1162, STM447, STM1416, STM342, STM062, STM149, STM1811, STM1774, STM1262, STM1827, STM1803, STM2116, STM1452, STM1542, STM2064, STM1730, STM1899, STM2147, STM2154, STM1954, STM2039, STM2163, STM1534, STM1775, and STM803). For example, as shown in Appendix 2 Figure 5, panel B, an isolate in a wild bird clade might be transmitted to a swine host (STM649). By PP, the swine label of the transmitted isolate would lead to an incorrect swine prediction of its neighboring isolate (STM204) in the original wild bird clade. RF prediction by contrast was not affected because it was based on the strong wild bird signal of STM204 and the rest of the wild bird isolates in the clade.

Another 6 isolates were correctly predicted by RF despite falling into a mixed-source clade (STM477, STM398, STM179, STM155, STM835 and STM284). One example, STM477, is shown in Appendix 2 Figure 5, panel A. It was correctly predicted to be bovine by RF even though it was located in a diverse-source clade including poultry, wild bird, and swine. One additional outlier isolate (STM1945) was distantly related to any BPSW isolate but still correctly predicted by RF. These predictions suggested that the RF classifier was able to function in some cases where lack of phylogenetic references might present a challenge to source prediction by PP. These RF predictions were based on compositions of genetic features similar to those of the training genomes from the same source. The fact that the majority of top 50 predictor features used by RF were located on mobile genetic elements (Figure 4, panel B) indicates that genes that can be horizontally transferred may at least partially contribute to RF's superior performance in such cases.

Correct Source Prediction by PP but Incorrect by RF (n = 18)

Six isolates in this category were found in clades where isolates from both bovine and poultry were present (STM174, STM299, STM295, STM326, STM1232, STM1806). Nine isolates were located in clades that were dominated by isolates from a different source (STM324, STM301, STM456, STM1639, STM995, STM996, STM978, STM1035, and STM267). Such

cases could be explained by putative spillover events that involved >1 closely related isolates, which served as the phylogenetic reference for each other to allow source prediction by PP as shown by STM324 and STM517 in Appendix 2 Figure 5, panel C. Three bovine isolates (STM302, STM459, STM278) were incorrectly predicted by RF as poultry or swine in spite of falling into mostly bovine clades. Interference from nearby poultry or swine isolates carrying similar genetic features as the query bovine isolates in their respective clade may cause the incorrect RF predictions.

11. Evaluation of Human Host Prediction Using the Random Forest (RF) Classifier

We performed an evaluation on predicting human host of *S. enterica* Typhimurium isolates using the Random Forest (RF) classifier similar to a previous study reported by Lupolova et al. that was based on a Support Vector Machine (SVM) classifier (*28*). For this analysis, human clinical isolates in the dataset (n = 160) were used as a separate training class. Miscellaneous food isolates, which displayed similar phylogenetic diversity as human isolates, were also included in the new classier as a training class for comparison. Human, miscellaneous food along with the 4 original classes of BPSW made the 6 training classes for the new classifier. After excluding redundant genomes that were separated by <10 SNPs and sampled from the same source and location in the same calendar year, a total of 1,473 genomes were included in the training data set. The same sets of core genome SNPs (n = 1,882) and indels (n = 150) for the BPSW classifier were used for the new classifier. Accessory genes were identified from the training *S. enterica* Typhimurium genomes using Roary (*19*) and defined as genes present in <99% of the genomes. For any accessory gene, if its source prevalence (defined as the percentage of isolates from a particular source that had the gene) differed by <25% between its most and least prevalent sources including human, food and BPSW, the gene was considered to be an insufficiently source discriminatory feature and removed from the analysis. After removing these genes, a final set of 1,282 accessory genes were obtained, a moderate increase from the 1,105 used by the BPSW classifier due to the inclusion of human and food isolates in the training data set. The RF classifier was built using the randomForest package (v4.6-12) (*28*) of R (*27*). The “ntree” argument was set to be 1,000 and default settings were used for other parameters. To estimate prediction errors, the RF algorithm used out of the bag (OOB) samples created by bootstrap aggregating or bagging of training data (*21*).

Preliminary evaluation of prediction accuracy for human host and miscellaneous food was 36.9% and 47.6% (excluding G1) respectively, compared with that between 50% and 90% for BPSW sources. The definition of the miscellaneous food source in this study included any food items other than retail meats. As the result, the food class defined here did not represent a singular and coherent reservoir of *S. enterica* Typhimurium. It was instead an aggregation of many food vehicles, of which any particular type did not have enough isolates to qualify as a single source class. Therefore, the low source prediction accuracy for food was likely the result of the inclusive classification of food. Human infections of *S. enterica* Typhimurium are mostly foodborne and *S. enterica* Typhimurium isolates should consequently reflect the diversity of miscellaneous food isolates, assuming *S. enterica* Typhimurium isolates circulating in foods are commonly virulent to humans. Human isolates in this study were indeed diverse and present in every population group along with miscellaneous food isolates, which explained the similarly low prediction accuracy for the human source.

12. Distribution of Acquired Antimicrobial Resistance Genes Among Zoonotic Sources of *S. enterica* Typhimurium

Antimicrobial resistance genes (ARGs) were identified from each of the 1,267 *S. enterica* Typhimurium genomes using the ResFinder database v3.0 (*29*). Each allele in the database was aligned to an *S. enterica* Typhimurium genome using BLAST. The presence of an ARG allele in the query genome was determined using default ResFinder setting. If an ARG type includes multiple alleles that showed at least 90% sequence similarity with each other, the alleles were clustered and 1 representative allele was used for alignment with the query genome. The distribution of detected ARGs among *S. enterica* Typhimurium genomes was shown in Appendix 2 Figure 6. Hierarchical clustering of detected ARGs was performed using the hclust package (*30*) of R (*27*). Distribution and clustering patterns of ARGs appeared to vary among zoonotic sources of *S. enterica* Typhimuiurm. Notably, ARGs were much less abundant in the wild bird clade compared with livestock clades. Antibiotic use in livestock may be related to the higher occurrence of ARGs in *S. enterica* Typhimurium isolates from livestock sources.

13. Different Levels of Human Isolate Clonality Between the Current and a Previous Machine Learning Classifier for *S. enterica* Typhimurium Source Prediction

While the RF classifier developed in this study and a Support Vector Machine (SVM) classifier reported in a previous study (*28*) both performed well in predicting livestock hosts or sources of *S. enterica* Typhimurium, their performances in predicting the human host of *S. enterica* Typhimurium genomes differed. Our RF classifier produced a host prediction accuracy of 36.9% for human isolates in our dataset compared with that of >90.0% by the SVM classifier using a different dataset. To investigate the cause of this difference, we compared the levels of human isolate clonality between the 2 studies. We constructed a maximum-likelihood tree based on core genome alignment of all the *S. enterica* Typhimurium genomes included in each study using Parsnp (*9*). As shown in Appendix 2 Figure 7, a total of 318 human isolates were included in the training set of the SVM classifier, most of which were clustered in 2 major clades. By contrast, a total of 160 human isolates used in the current study were scattered throughout the tree, with no visible clustering of many isolates except the Sub-Saharan Africa ST313 clade.

To exclude the possibility that the low accuracy in human host prediction was caused by the choice of RF as the machine learning classifier in the current study, we repeated the human host prediction analysis using SVM. We built a SVM classifier based on pan-genome gene content similar to the previously described approach (*28*) using the training set of the current study. Human and BPSW sources were included in the SVM classifier. The host prediction accuracy for human isolate was even lower at 13.5% by SVM compared with that of 36.9% by RF (or 35.6% if miscellaneous food isolates were excluded from the training set) (Appendix 1 Table 11). Similarly, SVM's performance in predicting BPSW source was lower than that of RF (Appendix 1 Table 11). In contrast with the systemic difference in performance between the 2 classifiers when applied to the current dataset, the relative difference between BPSW source prediction and human host prediction within a classifier was similar, with SVM being 46.6% and RF being 43.0% (Appendix 1 Table 11). These observations suggest that it was the dataset instead of the prediction algorithm that caused the difference in human host prediction between the current and the previous studies. Over-representation of clonally closely related isolates from a particular source in the training set can inflate the accuracy of machine learning-based

attribution to the source. As practiced in the current study, selection of phylogenetically diverse isolates and reduction of phylogenetic and epidemiological redundancy in the training set can help improve the performance of the source attribution model.

References

1. Bolger AM, Lohse M, Usadel B. Trimmomatic: a flexible trimmer for Illumina sequence data. Bioinformatics. 2014;30:2114–20. PubMed http://dx.doi.org/10.1093/bioinformatics/btu170

2. Bankevich A, Nurk S, Antipov D, Gurevich AA, Dvorkin M, Kulikov AS, et al. SPAdes: a new genome assembly algorithm and its applications to single-cell sequencing. J Comput Biol. 2012;19:455–77. PubMed http://dx.doi.org/10.1089/cmb.2012.0021

3. Gurevich A, Saveliev V, Vyahhi N, Tesler G. QUAST: quality assessment tool for genome assemblies. Bioinformatics. 2013;29:1072–5. PubMed http://dx.doi.org/10.1093/bioinformatics/btt086

4. Kurtz S, Phillippy A, Delcher AL, Smoot M, Shumway M, Antonescu C, et al. Versatile and open software for comparing large genomes. Genome Biol. 2004;5:R12. PubMed http://dx.doi.org/10.1186/gb-2004-5-2-r12

5. Zhou Y, Liang Y, Lynch KH, Dennis JJ, Wishart DS. PHAST: a fast phage search tool. Nucleic Acids Res. 2011 Jul;39(Web Server issue):W347-52.

6. Croucher NJ, Page AJ, Connor TR, Delaney AJ, Keane JA, Bentley SD, et al. Rapid phylogenetic analysis of large samples of recombinant bacterial whole genome sequences using Gubbins. Nucleic Acids Res. 2015;43:e15. PubMed http://dx.doi.org/10.1093/nar/gku1196

7. Didelot X, Wilson DJ. ClonalFrameML: efficient inference of recombination in whole bacterial genomes. PLOS Comput Biol. 2015;11:e1004041. PubMed http://dx.doi.org/10.1371/journal.pcbi.1004041

8. Price MN, Dehal PS, Arkin AP. FastTree 2—approximately maximum-likelihood trees for large alignments. PLoS One. 2010;5:e9490. PubMed http://dx.doi.org/10.1371/journal.pone.0009490

9. Treangen TJ, Ondov BD, Koren S, Phillippy AM. The Harvest suite for rapid core-genome alignment and visualization of thousands of intraspecific microbial genomes. Genome Biol. 2014;15:524. PubMed http://dx.doi.org/10.1186/s13059-014-0524-x

10. Corander J, Marttinen P, Sirén J, Tang J. Enhanced Bayesian modelling in BAPS software for learning genetic structures of populations. BMC Bioinformatics. 2008;9:539. PubMed http://dx.doi.org/10.1186/1471-2105-9-539

11. Li H, Durbin R. Fast and accurate long-read alignment with Burrows-Wheeler transform. Bioinformatics. 2010;26:589–95. PubMed http://dx.doi.org/10.1093/bioinformatics/btp698

12. Garrison E, Marth G. Haplotype-based variant detection from short-read sequencing. arXiv preprint arXiv:12073907. 2012.

13. Guindon S, Dufayard JF, Lefort V, Anisimova M, Hordijk W, Gascuel O. New algorithms and methods to estimate maximum-likelihood phylogenies: assessing the performance of PhyML 3.0. Syst Biol. 2010;59:307–21. PubMed http://dx.doi.org/10.1093/sysbio/syq010

14. Rambaut A, Lam TT, Max Carvalho L, Pybus OG. Exploring the temporal structure of heterochronous sequences using TempEst (formerly Path-O-Gen). Virus Evol. 2016 Jan;2(1):vew007.

15. Drummond AJ, Suchard MA, Xie D, Rambaut A. Bayesian phylogenetics with BEAUti and the BEAST 1.7. Mol Biol Evol. 2012;29:1969–73. PubMed http://dx.doi.org/10.1093/molbev/mss075

16. Suchard MA, Weiss RE, Sinsheimer JS. Bayesian selection of continuous-time Markov chain evolutionary models. Mol Biol Evol. 2001;18:1001–13. PubMed http://dx.doi.org/10.1093/oxfordjournals.molbev.a003872

17. Narzisi G, O'Rawe JA, Iossifov I, Fang H, Lee YH, Wang Z, et al. Accurate de novo and transmitted indel detection in exome-capture data using microassembly. Nat Methods. 2014;11:1033–6. PubMed http://dx.doi.org/10.1038/nmeth.3069

18. Choi Y, Chan AP. PROVEAN web server: a tool to predict the functional effect of amino acid substitutions and indels. Bioinformatics. 2015;31:2745–7. PubMed http://dx.doi.org/10.1093/bioinformatics/btv195

19. Page AJ, Cummins CA, Hunt M, Wong VK, Reuter S, Holden MT, et al. Roary: rapid large-scale prokaryote pan genome analysis. Bioinformatics. 2015;31:3691–3. PubMed http://dx.doi.org/10.1093/bioinformatics/btv421

20. Seemann T. Prokka: rapid prokaryotic genome annotation. Bioinformatics. 2014;30:2068–9. PubMed http://dx.doi.org/10.1093/bioinformatics/btu153

21. Breiman L. Out-of-bag estimation 1996.

22. Okoro CK, Kingsley RA, Connor TR, Harris SR, Parry CM, Al-Mashhadani MN, et al. Intracontinental spread of human invasive *Salmonella* Typhimurium pathovariants in sub-Saharan Africa. Nat Genet. 2012;44:1215–21. PubMed http://dx.doi.org/10.1038/ng.2423

23. Kingsley RA, Kay S, Connor T, Barquist L, Sait L, Holt KE, et al. Genome and transcriptome adaptation accompanying emergence of the definitive type 2 host-restricted *Salmonella enterica* serovar Typhimurium pathovar. MBio. 2013;4:e00565–13. PubMed http://dx.doi.org/10.1128/mBio.00565-13

24. Wu J, Mao X, Cai T, Luo J, Wei L. KOBAS server: a web-based platform for automated annotation and pathway identification. Nucleic Acids Res. 2006;34(Web Server issue):W720-4.

25. Kanehisa M, Goto S. KEGG: kyoto encyclopedia of genes and genomes. Nucleic Acids Res. 2000;28:27–30. PubMed http://dx.doi.org/10.1093/nar/28.1.27

26. Oksanen J, Kindt R, Legendre P, O'Hara B, Stevens MHH. The vegan Package. 2007.

27. Ihaka R, Gentleman R. R: a language for data analysis and graphics. J Comput Graph Stat. 1996;5:299–314.

28. Lupolova N, Dallman TJ, Holden NJ, Gally DL. Patchy promiscuity: machine learning applied to predict the host specificity of *Salmonella enterica* and *Escherichia coli*. Microb Genom. 2017;3:e000135. PubMed http://dx.doi.org/10.1099/mgen.0.000135

29. Kleinheinz KA, Joensen KG, Larsen MV. Applying the ResFinder and VirulenceFinder web-services for easy identification of acquired antibiotic resistance and *E. coli* virulence genes in bacteriophage and prophage nucleotide sequences. Bacteriophage. 2014;4:e27943. PubMed http://dx.doi.org/10.4161/bact.27943

30. Galili T. Hierarchical cluster analysis on famous data sets—enhanced with the dendextend package. 2018

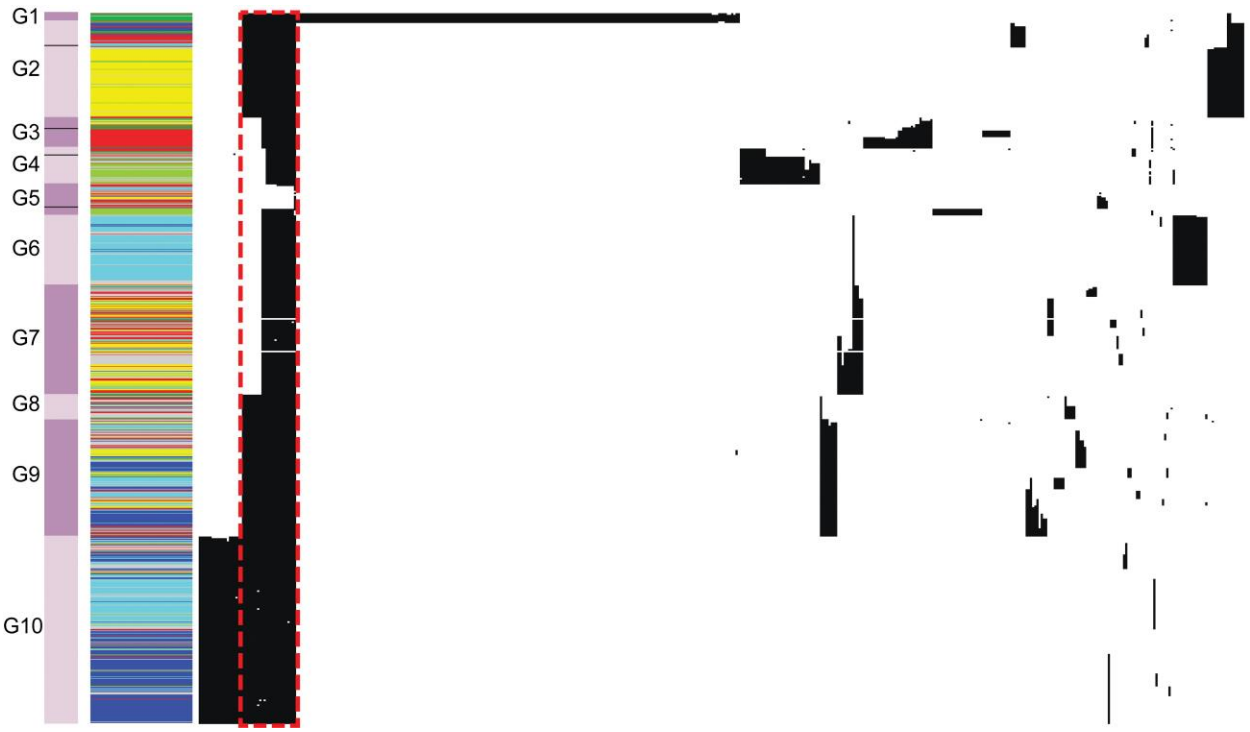

Appendix Figure 1. Distribution of nonsynonymous single-nucleotide polymorphisms and indels among *Salmonella enterica* Typhimurium genomes. *S. enterica* Typhimurium isolates are color coded by source and organized in the same order as they appear in the maximum-likelihood phylogeny (Figure 1, panel A). Cyan, yellow, light green, blue, dark green, red, and grey represents bovine, poultry, wild bird, swine, miscellaneous food, human, and other source, respectively.

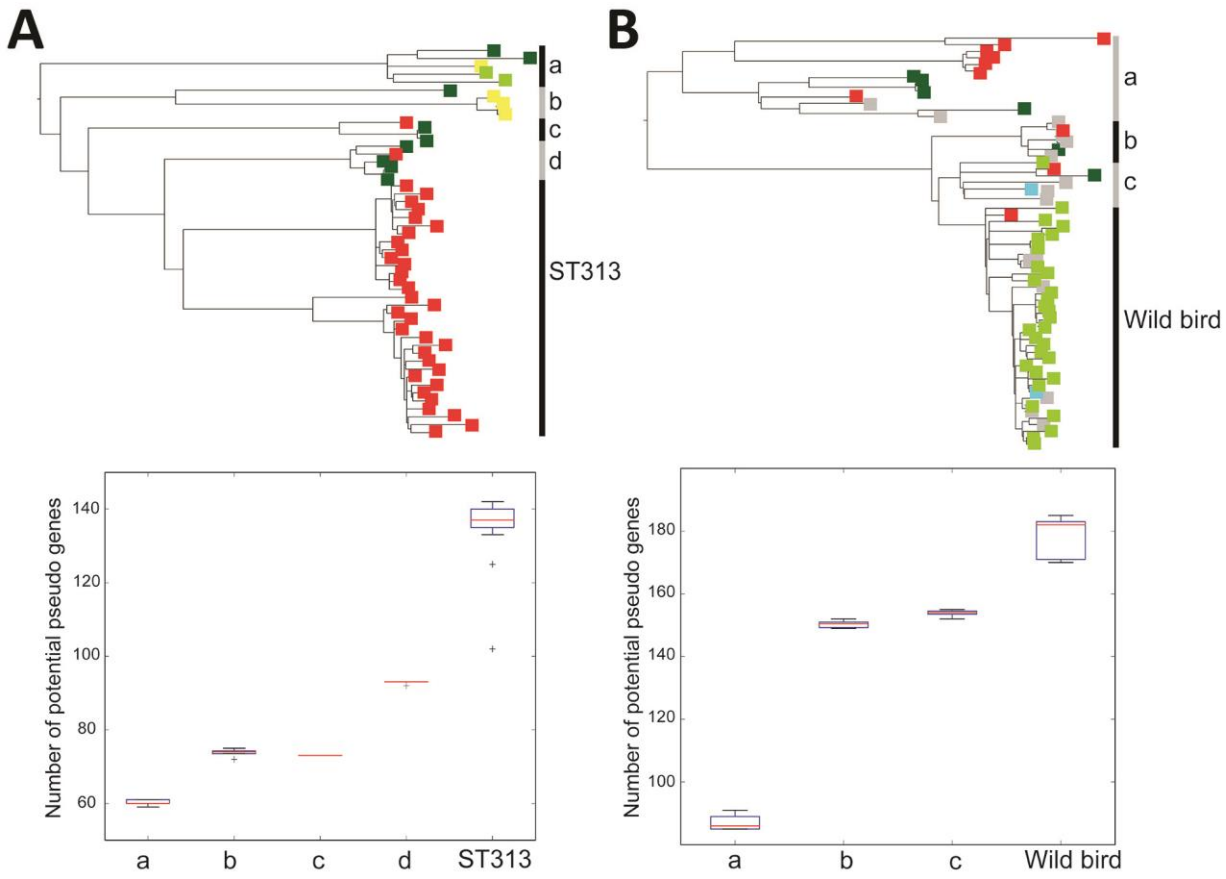

Appendix Figure 2. Examples of elevating accumulation of putative pseudogenes during potential host adaptation. A) The ST313 clade (upper) and putative pseudogene accumulation as it diverged from diverse-source clades (lower). B) Wild bird clade and putative pseudogene accumulation as it diverged from diverse-source clades. Both clades are subtrees of the *S. enterica* Typhimurium phylogeny of 1,267 isolates (Figure 1, panel A). Isolates on the trees are color coded by source (same as Figure 1, panel A): red, humans; dark green, food; yellow, poultry; light green, wild bird; cyan, bovine; blue, swine; grey, other sources.

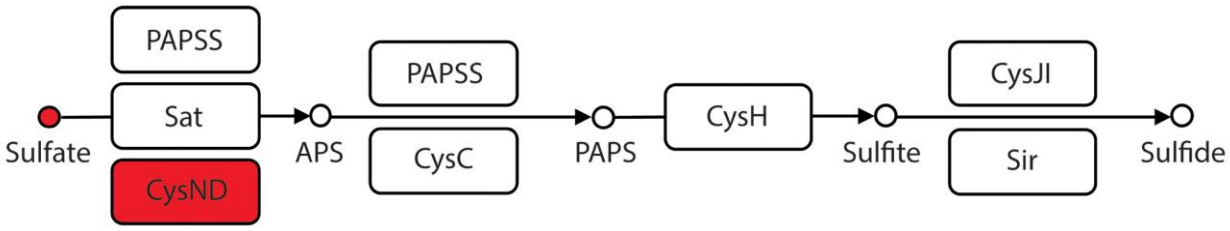

Appendix Figure 3. Assimilatory sulfate reduction pathway potentially disrupted by a nonsynonymous single-nucleotide polymorphism in a sulfate adenylyltransferase subunit gene (*cysN*). PAPSS, 3′-phosphoadenosine 5′-phosphosulfate synthase; Sat, sulfate adenylyltransferase; APS, adenosine-5′-phosphosulfate; PAPS, 3′-phosphoadenosine-5′-phosphosulfate; CysC, adenylylsulfate kinase; CysH, phosphoadenosine phosphosulfate reductase; CysJI, sulphite reductase flavoprotein (CysJ) and haem protein (CysI) subunits; Sir, sulfite reductase.

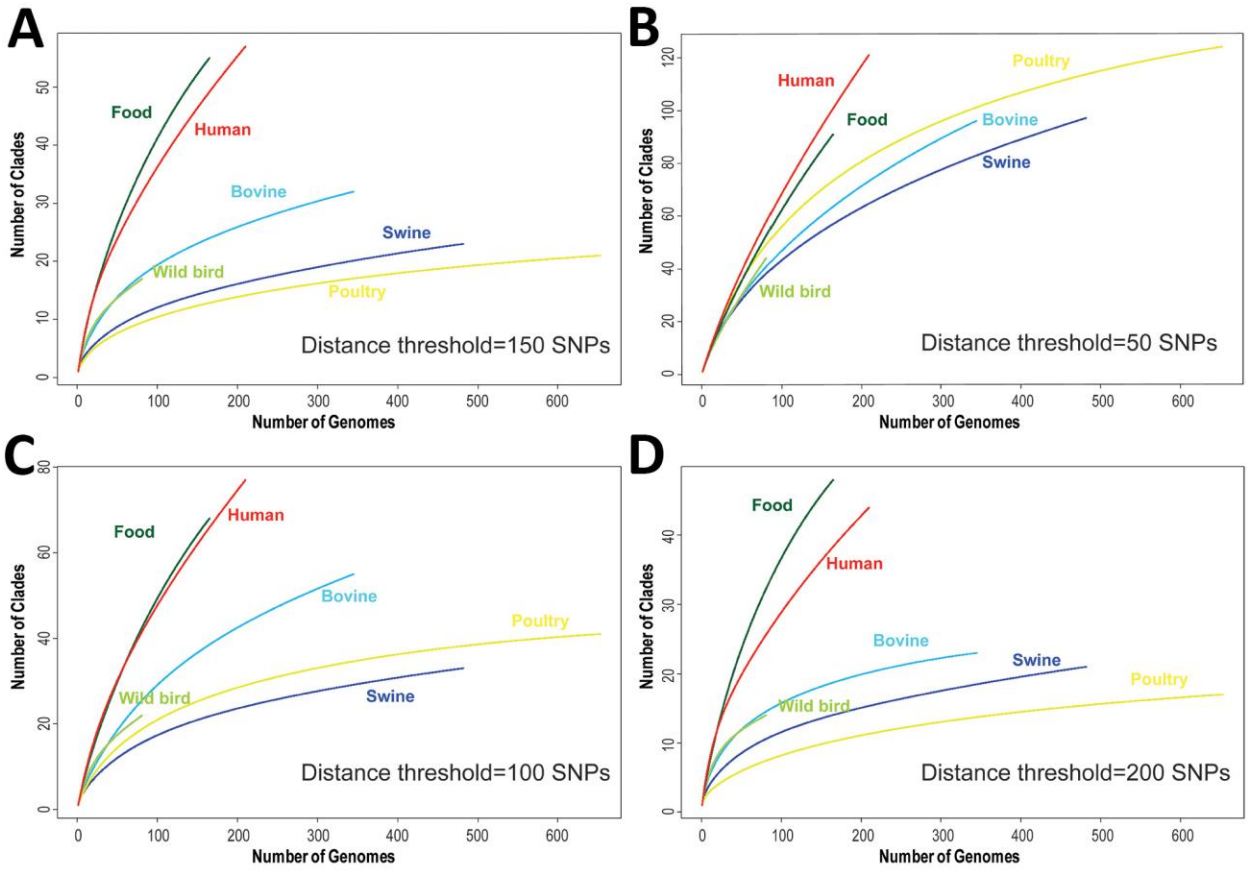

Appendix Figure 4. Rarefaction analysis relative sampling intensities by source. Each panel shows the result by adopting a particular single-nucleotide polymorphism distance threshold for defining phylogenetic clusters.

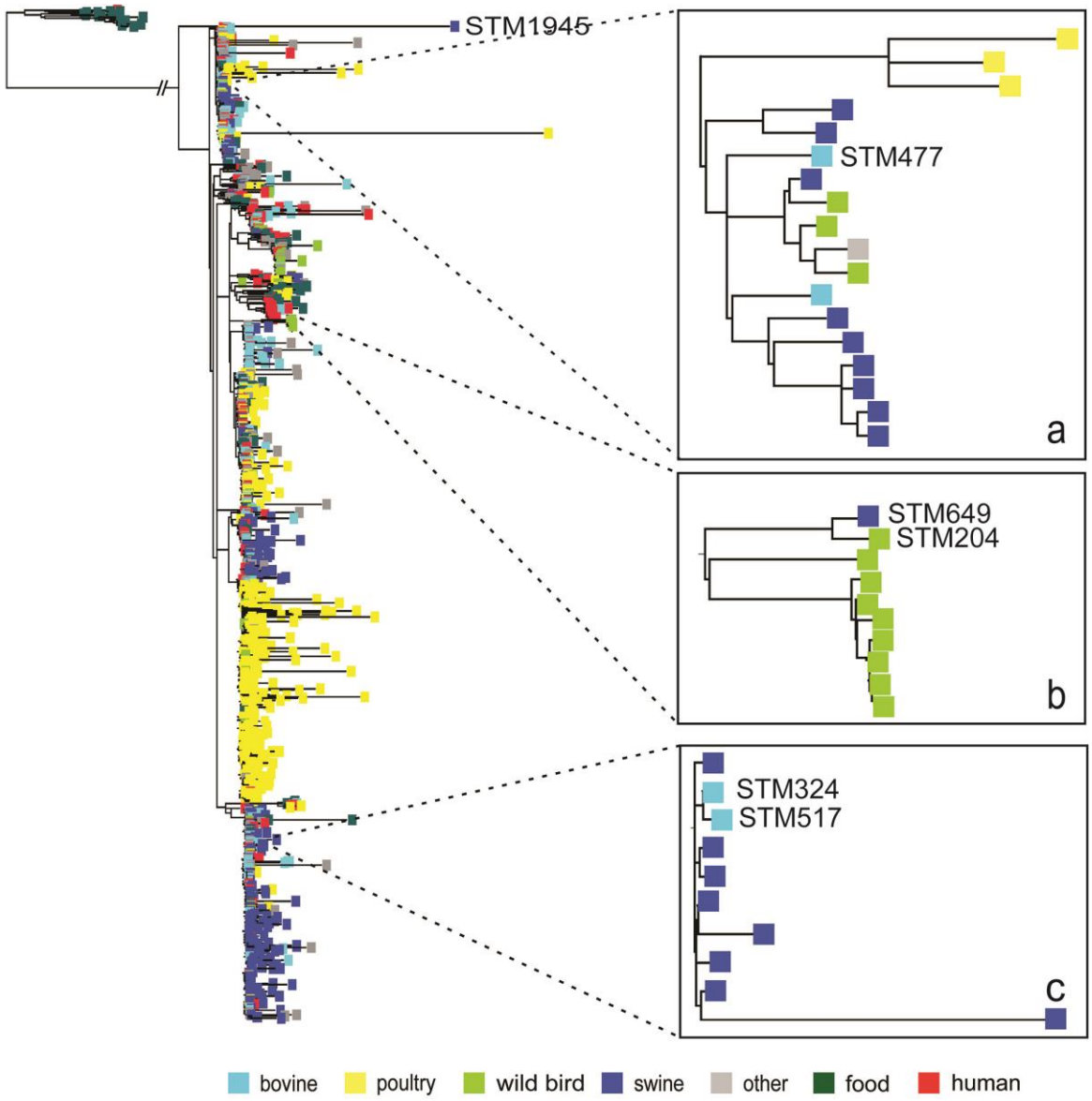

Appendix Figure 5. Examples of *Salmonella enterica* Typhimurium zoonotic source prediction by phylogenetic placement and Random Forest classifier. A total of 1,473 genomes were included in the tree. The original 1,267 *S. enterica* Typhimurium genome dataset for phylogenomic analyses was updated by 1) adding 939 *S. enterica* Typhimurium genomes that became available in GenomeTrakr from September 2015 (initially 1,267 genomes) to January 2017; 2) sequencing another 11 *S. enterica* Typhimurium isolates from 5 outbreaks with confirmed livestock origin in the United States from 2007 to 2013, which, together with 6 livestock isolates from 3 outbreaks in the original data set, led to a total of 8 zoonotic outbreaks for retrospective source attribution; and 3) excluding 744 redundant genomes to minimize biases due to repeated sampling of closely related strains. The genome updates resulted in a modified *S. enterica* Typhimurium collection of 1,473 isolates for source prediction. The 3 panels show the highlighted clades on the phylogenetic tree.

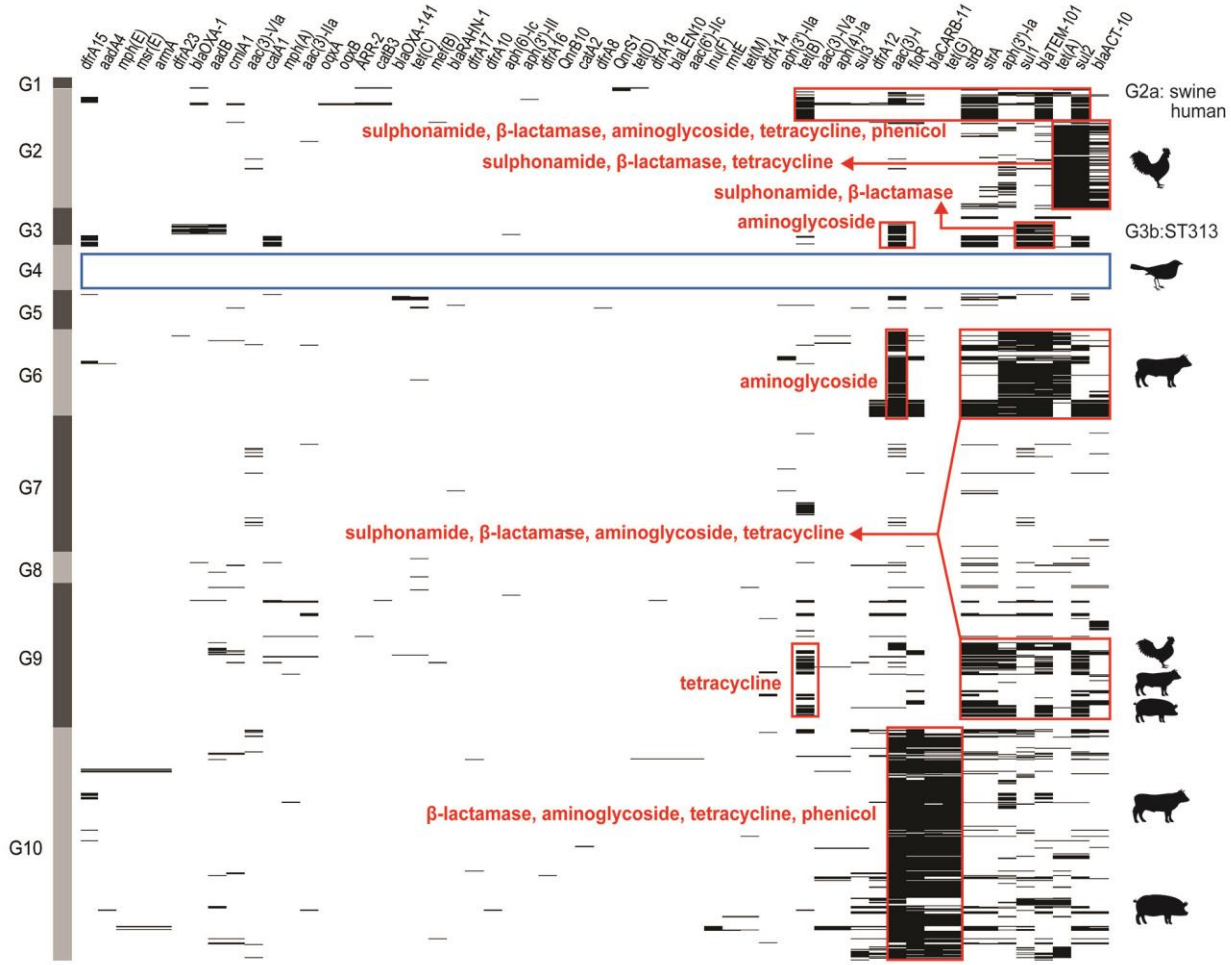

Appendix Figure 6. Distribution of antimicrobial resistance genes among *Salmonella enterica* Typhimurium genomes. Each black line stands for the presence of a specific gene. The vertical order of genomes is the same as that of the phylogenetic tree of 1,267 *S. enterica* Typhimurium genomes. Antimicrobial resistance gens surveyed and major population groups identified were labeled.

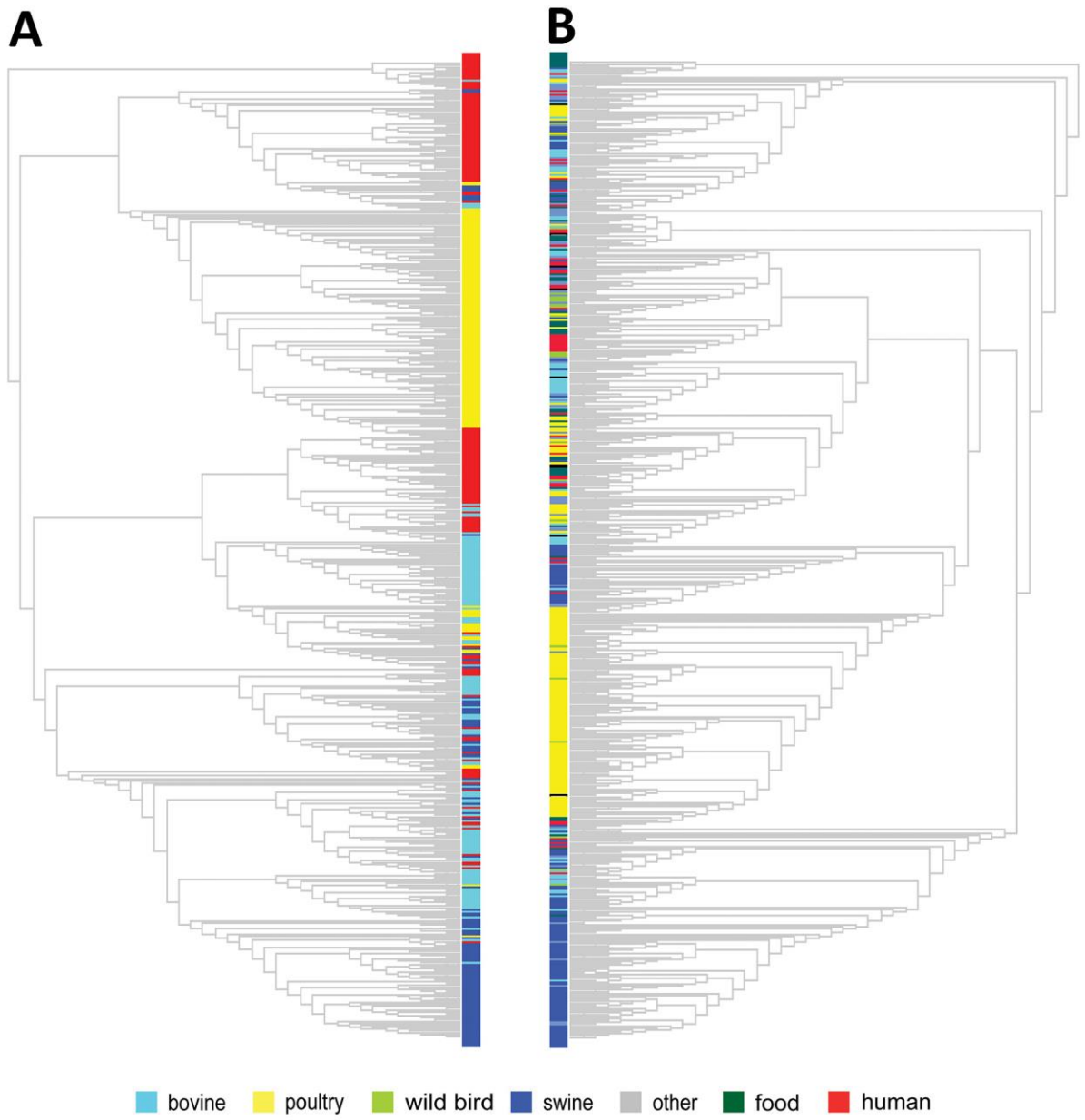

Appendix Figure 7. Comparison of human isolates clonality between the current and a previous study. A) Maximum-likelihood cladogram of *Salmonella enterica* Typhimurium genomes used for classifier training in a previous study based on core genome single-nucleotide polymorphisms. B) Maximum-likelihood cladogram of *S. enterica* Typhimurium genomes used for classifier training in the current study based on core genome single-nucleotide polymorphisms.